



저작자표시-비영리-변경금지 2.0 대한민국

이용자는 아래의 조건을 따르는 경우에 한하여 자유롭게

- 이 저작물을 복제, 배포, 전송, 전시, 공연 및 방송할 수 있습니다.

다음과 같은 조건을 따라야 합니다:



저작자표시. 귀하는 원저작자를 표시하여야 합니다.



비영리. 귀하는 이 저작물을 영리 목적으로 이용할 수 없습니다.



변경금지. 귀하는 이 저작물을 개작, 변형 또는 가공할 수 없습니다.

- 귀하는, 이 저작물의 재이용이나 배포의 경우, 이 저작물에 적용된 이용허락조건을 명확하게 나타내어야 합니다.
- 저작권자로부터 별도의 허가를 받으면 이러한 조건들은 적용되지 않습니다.

저작권법에 따른 이용자의 권리는 위의 내용에 의하여 영향을 받지 않습니다.

이것은 [이용허락규약\(Legal Code\)](#)을 이해하기 쉽게 요약한 것입니다.

[Disclaimer](#)

이학박사학위논문

화합물을 이용한 **Tau** 응집 조절과
응집된 **Tau** 에 세포막 결합에 대한
연구

**A study on novel inhibitor of Tau aggregation and
membrane binding of Tau aggregates**

2018 년 8 월

서울대학교대학원

생명과학부

최지현

A study on novel inhibitor of Tau aggregation and membrane binding of Tau aggregates

**By
Ji-Hyeon Choi**

**Advisor
Professor Sang-Hyun Park, Ph.D.**

A thesis for the Degree of Doctor of Philosophy

August 2018

School of biological Sciences

Seoul National University

A study on novel inhibitor of Tau aggregation and membrane binding of Tau aggregates

지도 교수 박 상 현

이 논문을 이학박사학위논문으로 제출함

2018년 7월

서울대학교 대학원

생명과학부

최 지 현

최 지 현 의 박사학위논문을 인준함

2018 년 7 월

위 원 장	<u>정 용 근 (인)</u>
부 위 원 장	<u>박 상 현 (인)</u>
위 원	<u>허 원 기 (인)</u>
위 원	<u>최 희 정 (인)</u>
위 원	<u>강 수 성 (인)</u>

A study on novel inhibitor of Tau aggregation and membrane binding of Tau aggregates

**A thesis submitted in partial fulfillment
of the requirement for the degree of**

DOCTOR of PHILOSOPHY

to the Faculty of

School of biological Sciences

at

Seoul National University

by

Ji Hyeon Choi

Date approved :

ABSTRACT

A study on novel inhibitor of Tau aggregation and membrane binding of Tau aggregates

Ji-Hyeon Choi

School of biological science

Seoul National University

Tau is an intracellular microtubule-associated protein that stabilizes microtubules. Under normal physiological conditions, Tau is a naturally unfolded and highly soluble protein. However, in Alzheimer's disease, Tau is hyperphosphorylated and aggregated into intracellular neurofibrillary tangles (NFT). Aggregated Tau can transmit into adjacent cells and induce aggregation. This prion-like Tau propagation is an important mechanism for disease progression. Therefore, inhibition of aggregation and transmission of Tau can provide an important strategy for therapeutic agents of Alzheimer's disease. In this study, we screened six novel inhibitors for Tau aggregation and designed one novel inhibitor based on the screened compounds structures. A total of 62 compounds were synthesized and 32

compounds efficiently inhibited Tau aggregation. Additionally, we developed a new measuring method for membrane binding of aggregated Tau. To measure aggregation-dependent membrane binding, fluorescence labeled Tau was utilized. Tau bound to living cell membranes by aggregation in a dose-dependent manner. In addition, using aggregation inhibitor, we confirmed that this method could be a convenient cell-based approach for validation or screening of membrane binding inhibitors.

Keywords : Tau, aggregation, Alzheimer's diseases, Inhibitor, Membrane binding, FACS, measurement

Student number : 2009-30089

COPYRIGHT INFORMATION

Portions of the dissertation have appeared in separate publication:

Ji-Hyeon Choi and Sang-Hyun Park. 2018. An iterative compound screening for identifying Tau aggregation inhibitors (preparing in submission).

Ji-Hyeon Choi and Sang-Hyun Park. 2018. Measurement membrane binding of Tau by using fluorescence (preparing in submission).

TABLE OF CONTENTS

	Page
ABSTRACT -----	i
COPYRIGHT INFORMATION -----	iii
TABLE OF CONTENTS -----	iv
LIST OF FIGURES -----	v
ABBREVIATION -----	xi
Chapter 1. -----	1
Screening compounds for Modulating of Tau aggregation	
INTRODUCTION -----	2
MATERIALS AND METHODS -----	4
Tau K18 purification -----	4
<i>In vitro</i> compound screening -----	5
Thioflavin T (ThT) fluorescence assay -----	5
Bis-ANS fluorescence assay -----	5
Transmission electron microscopy (TEM) -----	6
MTT reduction assay -----	6

RESULTS	8
Compound screening for Tau K18 aggregation	8
Compound scaffold for analog synthesis	8
Neutral red (NR) analogs	9
Phnylenediamine (PED) analogs	10
Thiazolidine (Thi) analogs	10
Dimethylphenzine (DMP) analogs	11
<i>De novo</i> scaffold (DN) analogs	11
Bis-ANS fluorescence assay	12
Cell viability assay	13
Filter-trapping assay	13
Inhibiting β-sheet formation during Tau K18 aggregation	14
Time-dependent disruption of β-sheet structure	15
DISCUSSION	26
Chapter 2.	82
Measurement membrane binding of Tau by using fluorescence	

INTRODUCTION	-----	83
MATERIALS AND METHODS	-----	85
Purification and labeling of recombinant Tau K18	---	85
<i>In vitro</i> Tau K18 aggregation	-----	86
SDS-PAGE analysis	-----	86
Thioflavin T (ThT) fluorescence assay	-----	87
Membrane binding analysis	-----	87
RESULTS	-----	89
Aggregation with the fluorescence labeled Tau K18	-----	89
Membrane binding of Tau K18 aggregates	-----	89
Aggregation state and dose-dependent membrane binding of Tau K18	-----	91
Binding of Tau K18 in various cell lines	-----	91
Membrane binding of α -synuclein aggregates	-----	93
DISCUSSION	-----	125
REFERENCES	-----	128
국문초록	-----	138

LIST OF FIGURES

	Page
Figure 1. Initial compound screening from 10K library -----	16
Figure 2. Categorized initial screened compound -----	18
Figure 3. Second screening for 106 compounds -----	20
Figure 4. Compound structure of final compounds -----	22
Figure 5. Scaffold compounds for analog synthesis -----	24
Figure 6. Synthesis scheme for neutral red (NR) analogs ----	26
Figure 7. ThT fluorescence intensity of incubating Tau K18 with NR analogs -----	28
Figure 8. Dose-dependent inhibition by neutral red (NR) analogues -----	30
Figure 9. Synthesis scheme for phenylenediamine (PED) analogues -----	32
Figure 10. ThT fluorescence intensity of incubating Tau K18 with PED analogues -----	34
Figure 11. Dose-dependent inhibition by PED analogues -----	36
Figure 12. Synthesis scheme for Thiazolidine (Thi) analogs -	38
Figure 13. ThT fluorescence intensity of incubating Tau K18 with Thi analogues -----	40
Figure 14. Synthesis scheme for Thiazolidine (Thi) analogs -	42
Figure 15. ThT fluorescence intensity of incubating Tau K18 with Thi analogues -----	44
Figure 16. Dose-dependent inhibition by Thiazolidine (Thi) analogues -----	46

Figure 17. Synthesis scheme for Dimethylphenazine (DMP) analogs	48
Figure 18. ThT fluorescence intensity of incubating Tau K18 with DMP analogs	50
Figure 19. Dose-dependent inhibition by DMP analog	52
Figure 20. Synthesis scheme for <i>De novo</i> (DN) scaffold analogs	54
Figure 21. ThT fluorescence intensity of incubating Tau K18 with DN analogs	56
Figure 22. Dose-dependent inhibition by DN analog	58
Figure 23. Bis-ANS fluorescence intensity of incubating Tau K18 with NR, PED, Thi analogs	60
Figure 24. Bis-ANS fluorescence intensity of incubating Tau K18 with DN analogs	62
Figure 25. Observing Tau aggregates with analogs by TEM	64
Figure 26. Reducing cytotoxicity of Tau K18 aggregates by analogs	66
Figure 27. Dose-dependent disruption aggregates by analogs	68
Figure 28. Time course of inhibition by NR, PED, DMP and Thi analogs	70
Figure 29. Time course of inhibition by DN analogs	72
Figure 30. Time course of disruption by NR, PED, DMP and	

Thi analogs -----	74
Figure 31. Time course of disruption by DN analogs -----	76
Figure 32. Working model of analogs on Tau K18 aggregation -----	78
Figure 33. Thioflavin T (ThT) fluorescence intensity of Tau K18 during aggregation -----	94
Figure 34. Sedimentation fraction of Tau K18 aggregates -----	96
Figure 35. Flow cytometer histogram of the membrane bound Tau K18 by incubation time -----	98
Figure 36. Membrane binding of Tau K18 in different buffer solutions -----	100
Figure 37. Flow cytometer histogram of membranes with remaining Tau K18 after the trypsin treatment -----	102
Figure 38. Fluorescence microscopy images showing the remaining Tau aggregates -----	104
Figure 39. Degradation of Tau K18 aggregates with trypsin -	106
Figure 40. Flow cytometer histogram of membrane bound Tau K18 by aggregation time -----	108
Figure 41. Flow cytometer histogram of membrane bound Tau K18 by treatment dose -----	110
Figure 42. ThT fluorescence of the inhibitor treated Tau K18 -----	112

Figure 43. Reducing membrane binding by EGCG	-----	114
Figure 44. Fluorescence microscope images showing the membrane bound Tau K18	-----	116
Figure 45. Cell line independent membrane binding of Tau K18	-----	118
Figure 46. Comparing Kd values of Tau aggregates and cells	-----	120
Figure 47 Aggregation kinetic α-synuclein in presence of fluorescence labeled α-synuclein	-----	122
Figure 48 Membrane binding of aggregated α-synuclein by treated dose	-----	124

ABBREVIATION

AD : Alzheimer's disease

FTDP-17 : Frontal temporal dementia linked to chromosome

NFT : Neurofibrillary tangles

CNS : Central nervous system

ThT : Thioflavin T

Bis-ANS : 4,4'-Dianilino-1,1'-Binaphthyl-5,5'-Disulfonic Acid

IPTG : isopropyl-D-thiogalactopyranoside

ODS : Octadecyl sulfate

MTT : 3-(4,5-Dimethylthiazol-2-yl)-2,5-Diphenyltetrazolium Bromide

NR : Neutral red

PED : Phnylenediamine

Thi : Thiazolidine

DMP : Dimethylphenzine

DN : *De novo* scaffold

EGCG : Epigallocatechin gallate

MB : Methylene blue

MTBR : Microtubule-binding domain

FACS : flow cytometry

DIC : Differential interference contrasts

PBS : Phosphatase buffered saline

NHS ester : Succinimidyl Ester

SDS-PAGE : Sodium dodecyl sulfate polyacrylamide gel electrophoresis

TBST : Tri-buffered saline tween 20

DMEM : Dulbecco's Modified Eagle's Media

FBS : Fetal bovine serum

HSPG : Heparan sulfate proteoglycans

Chapter 1

Screening a novel inhibitor of

Tau aggregation

INTRODUCTION

Alzheimer's disease (AD) is the leading cause of dementia and afflicts approximately 44 million people worldwide in the middle-aged and elderly population. In the brains of AD patients, Tau is aggregated into paired helical filaments that appear as intracellular neurofibrillary tangles and whose densities are directly related to disease severity and dementia¹⁻³. Tau is a microtubule-associated protein that is expressed as six isoforms in the human brain. These six isoforms of Tau differ from one another in containing 0N, 1N, or 2N amino-terminal inserts, and the presence of 3R or 4R microtubule-binding domain repeats⁴⁻⁵. Tau stabilizes microtubules, promotes the assembly of microtubules, and regulates the dynamic instability of microtubules, which allows reorganization of the cytoskeleton⁵⁻⁷. However, in AD patients, Tau dissociates from the microtubules and becomes prone to aggregate into paired helical filaments by abnormal hyperphosphorylation. This dissociation and aggregation suppresses microtubule regulation by Tau and leads to disruptions in cellular membranes, mitochondrial function, and protein homeostasis regulation⁷⁻¹⁰. Additionally, aggregated Tau can be transmitted to adjacent neurons in a variety of ways and induce

misfolding and aggregation of Tau similar to prion-like propagation¹¹⁻¹³. Recently, four main therapeutic approaches have been proposed as follows: inhibition of Tau hyperphosphorylation, stabilizing microtubules, inhibition of Tau aggregation, and clearance of pathological Tau⁴⁻⁵. Among these approaches, the inhibition of hyperphosphorylation and aggregation of Tau are the more fundamental approaches for inhibiting the propagation of pathological Tau. To inhibit Tau hyperphosphorylation, kinase inhibitors have been tested in AD patients; however, these kinases have different substrates to Tau. Inhibiting hyperphosphorylation of these other substrates can cause side effects. Tideglusib, which is an inhibitor of glycogen synthase kinase 3 β and is a typical kinase for Tau, has been tested in mild-to-moderate AD patients but produced no clinical benefit^{5, 14}. Conversely, a derivative of Methylene blue that is a Tau aggregation inhibitor did produce treatment benefits^{5, 15}. Additionally, various substances such as compounds¹⁶⁻¹⁷, peptides¹⁸⁻¹⁹ and nanoparticles²⁰⁻²¹ are being studied to assist in inhibition of Tau aggregation, which is a more promising therapeutic approach for AD patients.

In the present study, we screened a novel inhibitor of Tau aggregation. *In vitro* screening based on thioflavin T (ThT) was performed for a 10K compound library and various analogs were synthesized based on the

screened compounds. Synthesized analogs were characterized by secondary structure analysis (ThT and Bis-ANS), cytotoxicity assay of Tau aggregates, and transmission electron microscopy (TEM).

MATERIALS AND METHODS

Tau K18 purification

The Tau K18 fragment, comprising the Tau repeat domain and tagged with a N-terminal His6-tag, was cloned into pET-16b. The plasmid was transformed in BL21(DE3)/RIL. Transformants were grown in LB media at 37°C until OD₆₀₀ reached 0.8. Recombinant Tau K18 expression was induced with 1 mM isopropyl-D-thiogalactopyranoside (IPTG) and further incubated for 2 hours at 37°C. Then, cells were harvested by centrifugation at 4,000 × *g* for 15 min and re-suspended in PBS buffer (5 mM DTT and 1 mM PMSF). Re-suspended cell pellets were sonicated and centrifuged at 16,000 × *g* for 15 min. Cleared lysate was passed through Ni Sepharose 6 Fast Flow resin (GE healthcare) and the bound recombinant Tau K18 was eluted with 250 mM imidazole. Finally, the purified recombinant protein was dialyzed using a Snakeskin dialysis tube (ThermoFisher) overnight against PBS buffer at 4°C with constant stirring to remove imidazole and degrade the fragment. The purified Tau K18 concentration was determined by OD₂₈₀ using an extinction coefficient of 4,080 M⁻¹cm⁻¹.

***In vitro* compound screening**

For initial screening, recombinant Tau K18 (10 μ M) and a library compound (20 μ M) were incubated in a 96-well plate (#32296, SPL) with constant shaking aggregation buffer (PBS, pH 7.4, 2 mM dithiothreitol, 50 μ M octadecyl sulfate). A second screening was conducted in Tau K18 (100 μ M) and compounds (10 μ M) in previously described buffer.

Thioflavin T (ThT) fluorescence assay

ThT was dissolved in PBS buffer to 1 mM and stored at 4°C. A total of 5 μ M of ThT was added to the aggregated sample and the fluorescence was measured in triplicate in white 96-well plates (31296, SPL) using a multilabel plate reader (EnVisoin, Perkin Elmer) at excitation and emission wavelengths of 440 and 485 nm, respectively.

Bis-ANS fluorescence assay

Bis-ANS was dissolved in PBS buffer to a concentration of 10 mM and stored at 4°C. A total of 5 μ M of Bis-ANS was added to the aggregated sample and the fluorescence was measured in triplicate in white 96-well plates (31296, SPL) using a multilabel plate reader (EnVisoin, Perkin Elmer) at excitation and emission wavelengths of

380 and 485 nm, respectively.

Transmission electron microscopy (TEM)

Aggregated Tau K18 was observed by TEM using a LIBRA 120 electron microscope (Carl Zeiss). Tau aggregation reaction mixtures containing Tau K18 (100 μ M), ODS (50 μ M), and compounds (10 μ M) were incubated at 37°C for 24 hours and applied to carbon grids followed by staining with 1% uranyl acetate. The electron microscope was operated at 100 kV and the grid was observed at 20,000 \times magnification.

MTT reduction assay

SH-SY5Y cells (neuroblastoma cell line) were cultured in DMEM with 10% fetal bovine serum (FBS) in a 5% CO₂ incubator at 37°C. Cells were inoculated at a density of 10,000 cells/well in 96-well plates. After 24 h, Tau K18 (100 μ M) aggregated with compounds (100 μ M) was presented to cells for 24 h. Then, 20 μ L of MTT solution (5 mg/mL) was added to each well and incubated for 2 hours.

Transmission electron microscopy (TEM)

Aggregated Tau K18 was observed by TEM using an electron

microscope LIBRA 120 (Carl Zeiss). Tau aggregation reaction mixtures containing Tau K18 (100 μ M), ODS (50 μ M) and compounds (10 μ M) were incubated at 37°C for 24 hours, and applied to carbon grids followed by staining with 1% uranyl acetate. Electron microscope was operated at 100 kV and the grid was observed at a $\times 20,000$ magnification.

MTT reduction assay

SH-SY5Y cells (neuroblastoma cell line) were cultured in DMEM with 10% FBS, in a 5% CO₂ incubator 37°C. Cells were inoculated at density of 10,000 cells/well in 96-wll plates. After 24H, Tau K18 (100 μ M) aggregated with compounds (100 μ M) was treated to cell for 24 hours. Then, 20ul of MTT solution (5mg/ml) was added to each well and incubated for 2 hours.

RESULTS

Screening inhibitor for Tau K18 aggregation

A 9,770 compound library consisting of 5,000 CNS penetrable compounds and 4,770 random compounds was prepared and screening of individual compounds to inhibit Tau aggregation was conducted using a ThT fluorescence assay. The ThT fluorescence assay is a representative method for confirming amyloidosis by reflecting the β -sheet structure formed during aggregation²²⁻²³. During the first screening, 106 compounds were identified that inhibited β -sheet formation by less than 70% compared to Tau K18 with DMSO (Figure 1). These 106 compounds were grouped into 15 clusters based on their substructure (Figure 2). A second screening was performed under more stringent conditions to exclude false and weak positives. A total of 17 compounds in clusters A, B, D, E, L, and N that inhibited β -sheet formation of Tau K18 below 50% successfully passed through the screening (Figures 3 and 4).

Compound scaffold for analog synthesis

Four compounds (D2, L1, L2, and N2) were finally selected as the

chemical scaffold for analog synthesis. Additionally, we designed *de novo* scaffolds (DN) based on the screened compounds (Figure 5). However, compounds in clusters A and B had high similarity to resveratrol, benzothiazole, and benzohydrazide, which are known to be effective aggregation inhibitors²⁴⁻²⁶ and the other two compounds (E1 and N1) were not suitable for synthesis of analogs.

Neutral red (NR) analogs

Based on the structure of NR, six analogs were synthesized by modifying the amines site to six residues (Figure 6). Among these analogs, NR, NR-1, and NR-2 modified with amines, trimethylamine, and N-ethyl-N-methylethanamine, respectively, significantly inhibited β -sheet formation and had similar IC₅₀ values (Figures 7 and 8). However, NR-3, NR-4, NR-5, and NR-6 modified with dimethylamine, N-methylethanamine, N-methylacetamide, and N-methylcyclopropanecarboxamide, respectively, did not inhibit β -sheet formation compared to DMSO (Figure 7). These results indicate that the amine site was one of the key sites for the inhibition of Tau aggregation.

Phenylenediamine (PED) analogs

Seven analogs were synthesized by modifying four sites in PED with four residues (Figure 9). Amines of R3 were important sites for inhibition and the analog modified with nitromethane did not inhibit the β -sheet formation (PED-4, 5, 6, and 7) (Figure 10). In addition, inhibition by the PED analog decreased as the number of modified methyl groups increased. The difference in IC₅₀ values between PED and PED-1 was due to one methyl group difference (Figure 11).

Thiazolidine (Thi) analogs

Thi analogs were synthesized in two groups. The first group changed five sites to six residues (Figure 12) and the second group changed six sites to six residues (Figure 14). Thi, Thi-2, Thi-6, and Thi-10 in the first group effectively inhibited the formation of the Tau K18 β -sheet structure. This result indicated that modification of the hydroxy residues in R1 and R3 was important, whereas the other site was not significant for inhibition (Figure 13). Similar trends were observed in the second group. Thi-13, Thi-14, Thi-15, and Thi-16, in which the hydroxyl residue was modified at two positions, showed efficient inhibitory effects in β -sheet formation (Figure 15). Thi-2, Thi-6, Thi-10, Thi-14, and Thi-15, in which the hydroxyl residue was modified in

two positions, had IC₅₀ values lower than those of Thi and Thi-13 (Figure 16). This result suggests that the hydroxyl group residue plays a role in improving the inhibitory effect of the Thi scaffold.

Dimethylphenazine (DMP) analogs

Seven analogs were synthesized by changing two sites to five residues in DMP (Figure 17). Modification of DMP residues reduced the inhibitory effect of Tau K18 β -sheet formation (Figure 18). IC₅₀ values of DMP-3 and DMP-5 were higher than those of DMP (Figure 19). Therefore, two amine residues of DMP were not suitable as modification sites.

***De novo* scaffold (DN) analogs**

DN was derived based on 17 compounds found through screening and 18 analogs were synthesized based on this scaffold (Figure 20). However, there was no significant difference in the inhibitory effect between synthesized analogs (Figure 21), which was reproduced in comparison with the IC₅₀ value (Figure 22). These results suggest that the inhibitory effect of the DN analogs was most affected by their scaffold structure and that the residue modification could not interfere with it.

Bis-ANS fluorescence assay and transmission electron microscopy (TEM) as a complementary assay

To better validate inhibition by analogs, it was necessary to combine other methods with the ThT fluorescence assay. We used the Bis-ANS fluorescence assay, TEM, and cell viability assay. The exposure of the hydrophobic regions and fibril formation during Tau aggregation were another important structural feature. Such exposures could be monitored by Bis-ANS fluorescent dye and has been widely utilized to monitor protein aggregation²²⁻²³. Tau K18 with analogs showed inhibited exposure at approximately 60%–70% compared with DMSO during aggregation and the different inhibition efficiencies between analogs was not significant except for Thi, Thi-13, and Thi-16 (Figures 23 and 24). Thi, Thi-13, and Thi-16 were also reduced by approximately 40% compared to DMSO. As a result, 24 analogs inhibited exposure of the hydrophobic region as well as ThT-based assay results. Next, the ultrastructure of Tau K18 aggregates was confirmed by TEM. TEM images showed the effect of analogs on fibril formation that occurred during Tau K18 aggregation. Tau K18 with DMSO formed fibrils after 24 h incubation; however, Tau K18 with NR, PED, Thi, and DMP significantly inhibited fibril formation (Figure 25).

Cytotoxicity of Tau aggregates

The cellular response by Tau K18 aggregates was validated. Extracellular aggregates such as synuclein, β -amyloid, and Tau displayed cytotoxicity by reducing mitochondrial activity and increasing ROS of cells²⁷⁻²⁸. Cell viability with Tau K18 aggregates was determined by the MTT assay. Tau K18 with DMSO reduced cell viability by approximately 30% (Figure 26). Thi, NR, PED, and DMP analogs, apart from Thi-13, reduced the toxicity of Tau aggregates. Additionally, DN analogs reduced toxicity except for five analogs (DN-10, DN-12, DN15, DN-16, and DN-17). Structure analysis using a fluorescent probe showed that inhibition by DN analogs was approximately 10 times higher than that of other derivatives such as NR, PED, Thi, and DMP (Figures 8, 11, 16, 19, and 22). However, reducing cytotoxicity by analogs was not significantly different. This difference showed that DN analogs inhibit cell viability or mitochondrial activity.

Disruption of Tau K18 aggregates by analogs

Resveratrol and benzothiazole were selected in our screening and can inhibit the aggregation of amyloid proteins as well as disrupt

aggregates^{26, 29}. We speculated that our screened inhibitors would also have such disruption effects. To verify this disruption, various concentrations of NR, PED-1, and DMP were treated to Tau K18 aggregates. NR, PED-1, and DMP efficiently disrupted Tau K18 aggregates with the disruption efficiency not being significantly different to inhibition. IC50 values of NR, PED, and DMP were 2 to 5 μM and DC50 values were also 2 to 5 μM (Figure 27).

Kinetics of inhibition and disruption of Tau K18 by analogs

Similar IC50 and DC50 values indicated that the inhibition and disruption by analogs occurred via similar processes. To validate this process, the aggregation of Tau K18 with analogs over time was monitored. Tau aggregation typically displays sigmoidal growth kinetics³⁰⁻³¹. Analog reduced overall aggregation by approximately 55% compared to DMSO (Figures 28 and 29); however, similar to DMSO, Tau K18 aggregation with analogs rapidly increased from 0 hour to 4 hours without a lag phase (Figures 28 and 29). This tendency shows that analogs did not affect either the lag phase or the elongation phase. When analogs were treated to Tau K18 aggregates, aggregates instantly induced structural changes and remained constant (Figures 30 and 31).

Figure 1. Initial compound screening from 10K library

Each compounds (20 μ M) in compound library were incubated with Tau K18 (10 μ M) for 6 hours. β -sheet formation of Tau K18 was measured by Thioflavin T(ThT) fluorescence assay. Each ThT fluorescence intensity was normalized by DMSO treated Tau K18. Dotted line represented inhibition cutoff indicating 70% inhibition. Compounds with value of less than 70% cutoff were used as targets for further screening

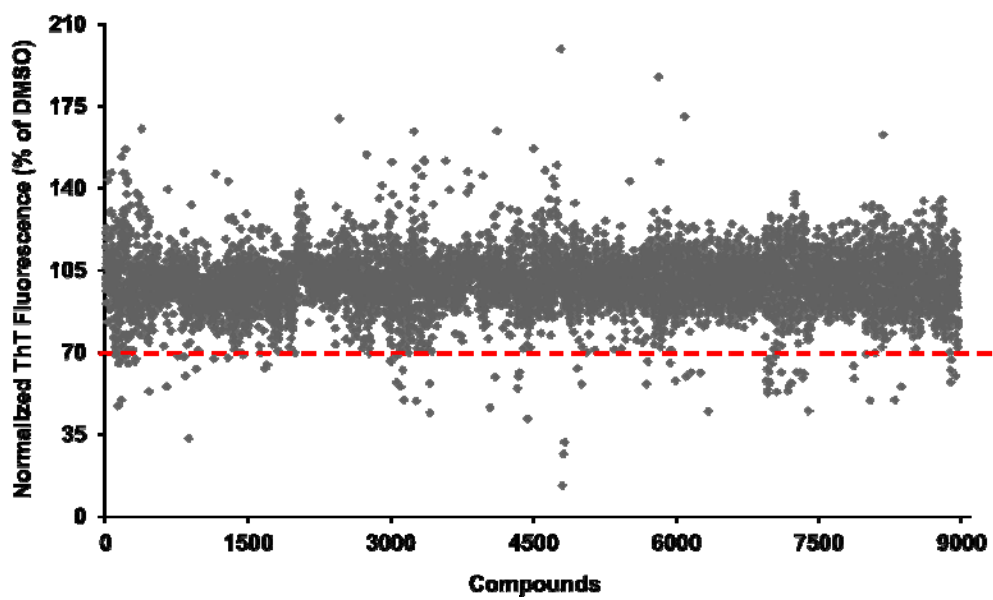


Figure 2. Categorized initial screened compound

Primary compounds (n = 106) from the initial screening were categorized by their chemical substructure.

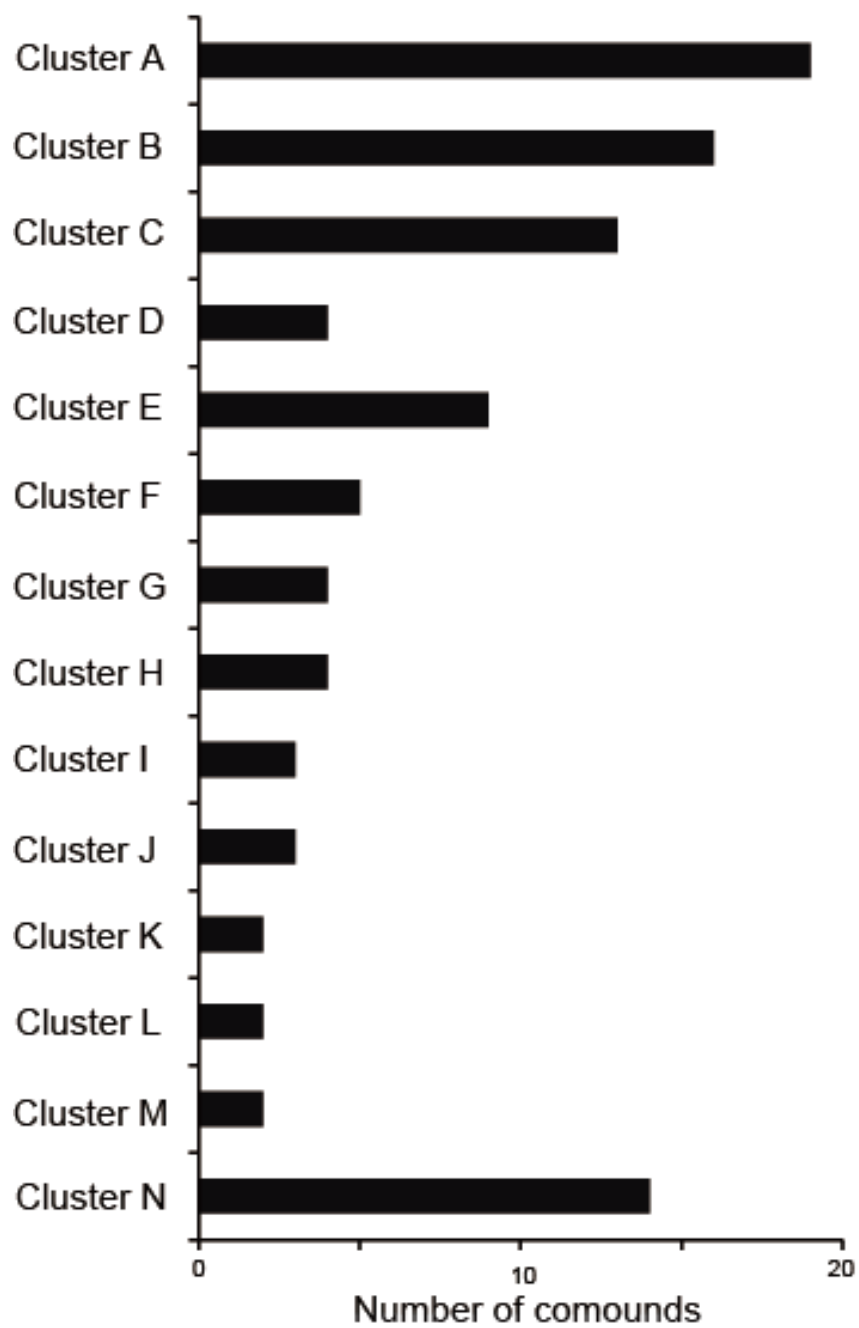


Figure 3. Second screening for 106 compounds

A second screening was performed under more stringent conditions for 106 primary compounds. Tau K18 (100 μ M) and 100 compounds (10 μ M) were incubated and Tau K18 aggregation was analyzed by ThT fluorescence.

Each ThT fluorescence intensity was normalized by DMSO-treated Tau K18. The dotted line represents the inhibitory cutoff, which showed 50% inhibition. Compounds with inhibition lower than the cutoff were selected as the final compounds for the aggregation inhibitors.

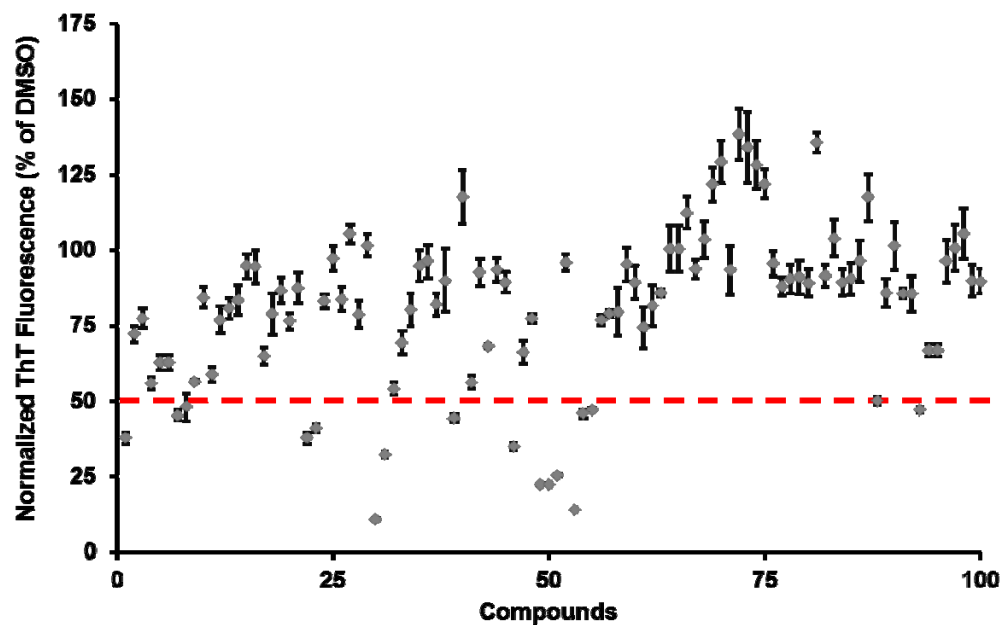


Figure 4. Compound structure of final compounds

Seventeen compounds were selected as the final compounds from 2nd screening

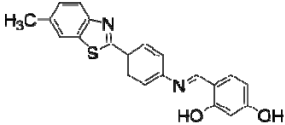
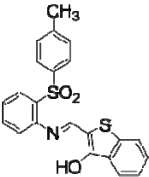
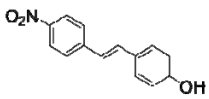
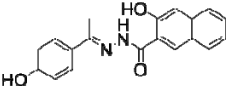
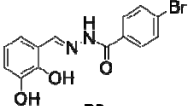
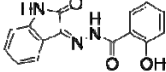
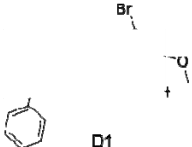
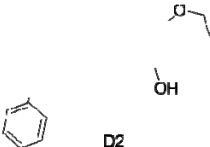
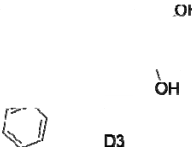
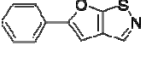
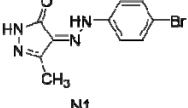
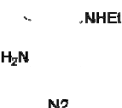
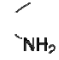
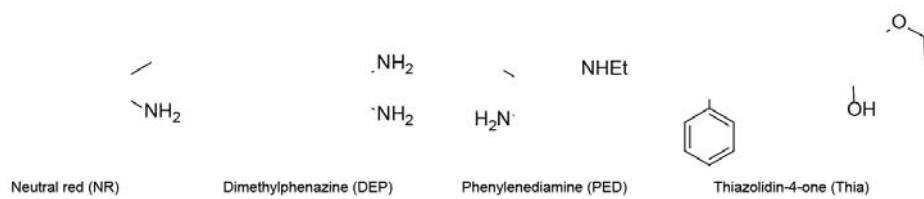
Cluster A	 <p>A1</p>	 <p>A2</p>	 <p>A3</p>
Cluster B	 <p>B1</p>	 <p>B2</p>	 <p>B3</p>
Cluster D	 <p>D1</p>	 <p>D2</p>	 <p>D3</p>
Cluster E	 <p>E1</p>	Cluster L	
Cluster N	 <p>N1</p>	 <p>N2</p>	 <p>N3</p>

Figure 5. Scaffold compounds for analog synthesis

(A) Four compounds were selected as the scaffold for synthesis analogs.

(B) *De novo* scaffold was designed based the 17 final compound compounds.

(A)



(B)

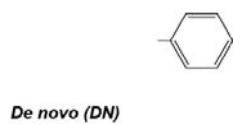


Figure 6. Synthesis scheme for neutral red (NR) analogs

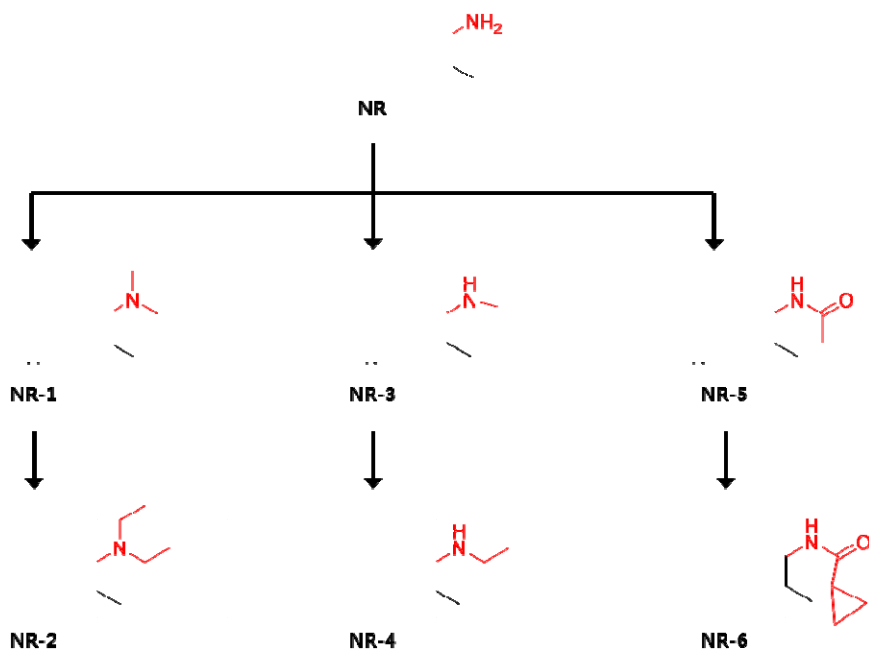
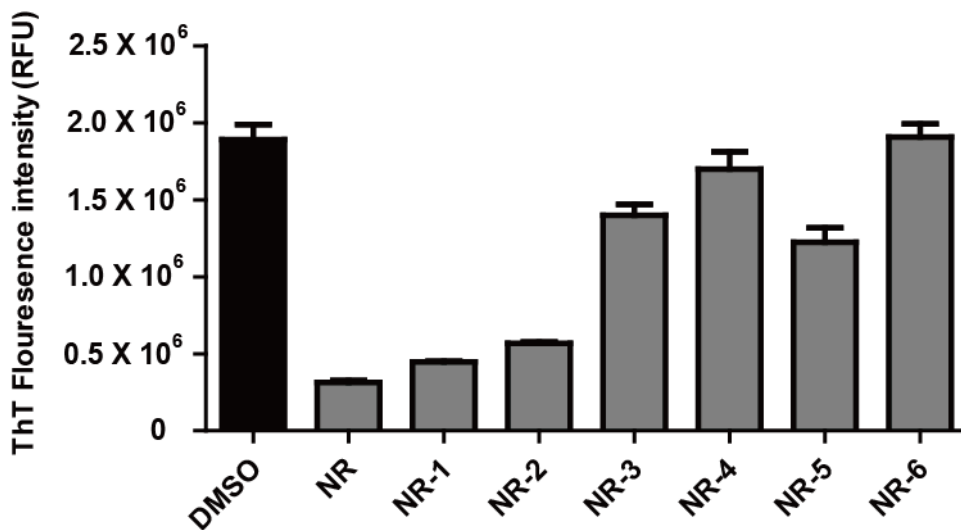


Figure 7. ThT fluorescence intensity of incubating Tau K18 with NR analogs

(A) To compare inhibition effects, neutral red (NR) analogs (10 μ M) were incubated with Tau K18 (100 μ M) for 6 hours and Tau K18 aggregation was measured ThT fluorescence assay. Each independent experiment was performed in triplicate; data are expressed as means \pm S.D

(B) Measured fluorescence intensity was normalized by DMSO treated Tau K18

(A)



(B)



Compounds	NR	NR-1	NR-2	NR-3	NR-4	NR-5	NR-6
R group	$-\text{NH}_2$	$-\text{N}(\text{CH}_3)_2$	$-\text{N}(\text{CH}_2\text{CH}_3)_2$	$-\text{N}(\text{CH}_3)\text{CH}_2\text{CH}_3$	$-\text{N}(\text{CH}_3)\text{CH}_2\text{CH}_2\text{CH}_3$	$-\text{N}(\text{CH}_3)\text{C}(=\text{O})\text{CH}_3$	$-\text{N}(\text{CH}_3)\text{C}(=\text{O})\text{C}_3\text{H}_5$
Aggregation (% of DMSO)	16.54 ± 0.69	23.63 ± 0.25	30.08 ± 0.34	74.06 ± 3.69	89.93 ± 6.03	64.78 ± 4.93	100.96 ± 4.44

Figure 8. Dose-dependent inhibition by neutral red (NR) analogs

Tau K18 (100 μ M) were incubated with various concentration of NR analogs (0.01, 0.1, 1, 10 and 100 μ M) and inhibition effect was measured by ThT assay. Measured fluorescence intensity was normalized by DMSO treated Tau K18.

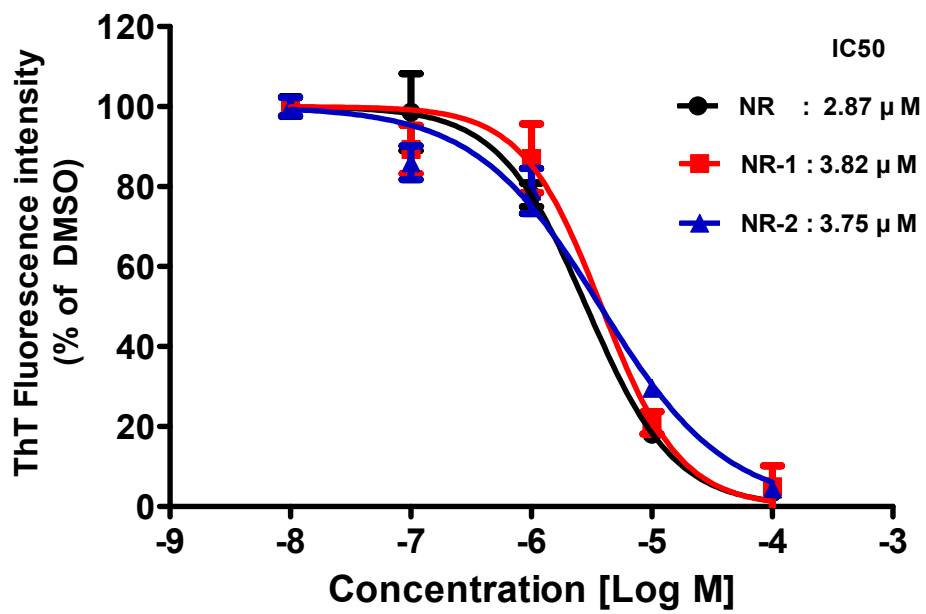


Figure 9. Synthesis scheme for phenylenediamine (PED) analogs

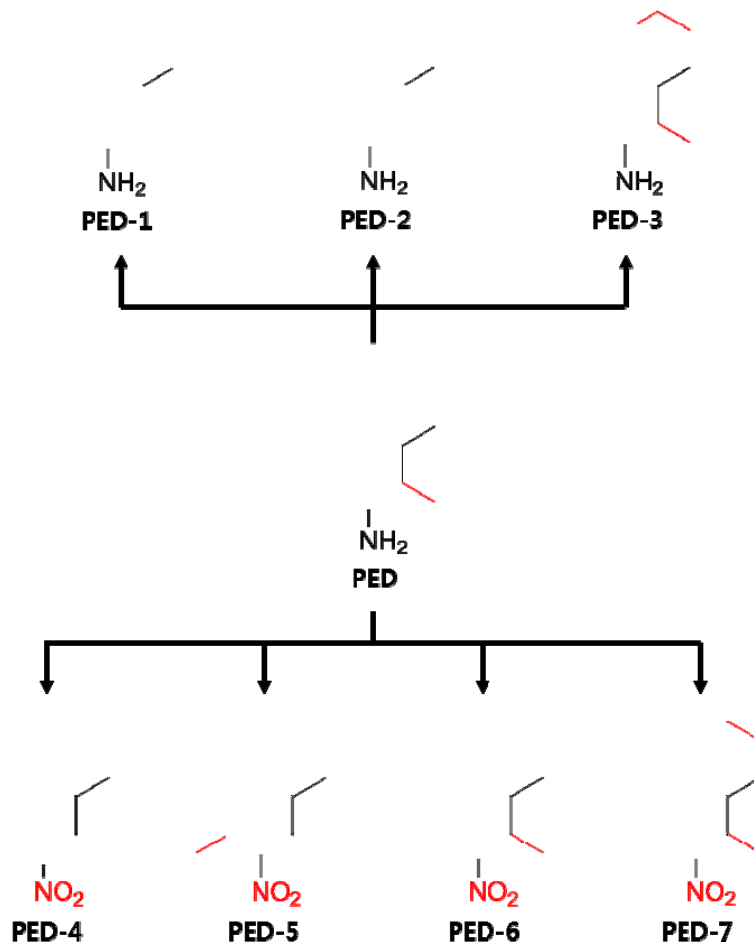
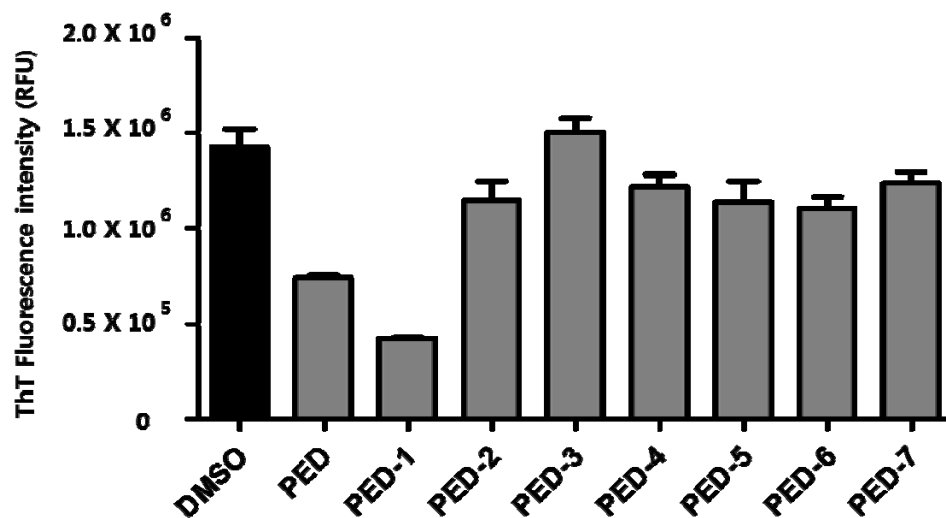


Figure 10. ThT fluorescence intensity of incubating Tau K18 with PED analogs

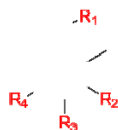
(A) To compare inhibition effects, phenylenediamine (PED) analogs (10 μ M) were incubated with Tau K18 (100 μ M) for 6 hours and Tau K18 aggregation was measured ThT fluorescence assay. Each independent experiment was performed in triplicate; data are expressed as means \pm S.D

(B) Measured fluorescence intensity was normalized by DMSO treated Tau K18

(A)



(B)



Compounds	PED	PED-1	PED-2	PED-3	PED-4	PED-5	PED-6	PED-7
R1 group	H	H	H		H	H	H	
R2 group	-CH ₃	H	H	-CH ₃	H		-CH ₃	-CH ₃
R3 group	-NH ₂	-NH ₂	-NH ₂	-NH ₂	-NO ₂	-NO ₂	-NO ₂	-NO ₂
R4 group	H	H	-CH ₃	H	H	-CH ₃	H	H
Aggregation (% of DMSO)	51.98 ± 0.88	29.66 ± 0.52	80.55 ± 7.18	105.68 ± 5.12	85.45 ± 4.58	79.82 ± 7.81	77.54 ± 4.34	86.93 ± 3.91

Figure 11. Dose-dependent inhibition by PED analogs

Tau K18 (100 μ M) were incubated with various concentration of PED analogs (0.01, 0.1, 1, 10 and 100 μ M) and inhibition effects were measured by ThT assay. Measured fluorescence intensity was normalized by DMSO treated Tau K18.

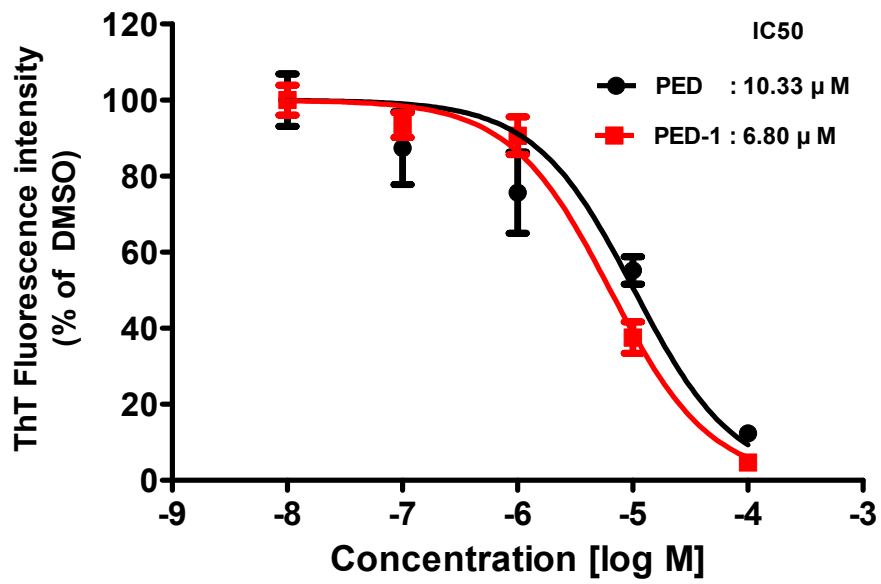


Figure 12. Synthesis scheme for thiazolidine (Thi) analogs

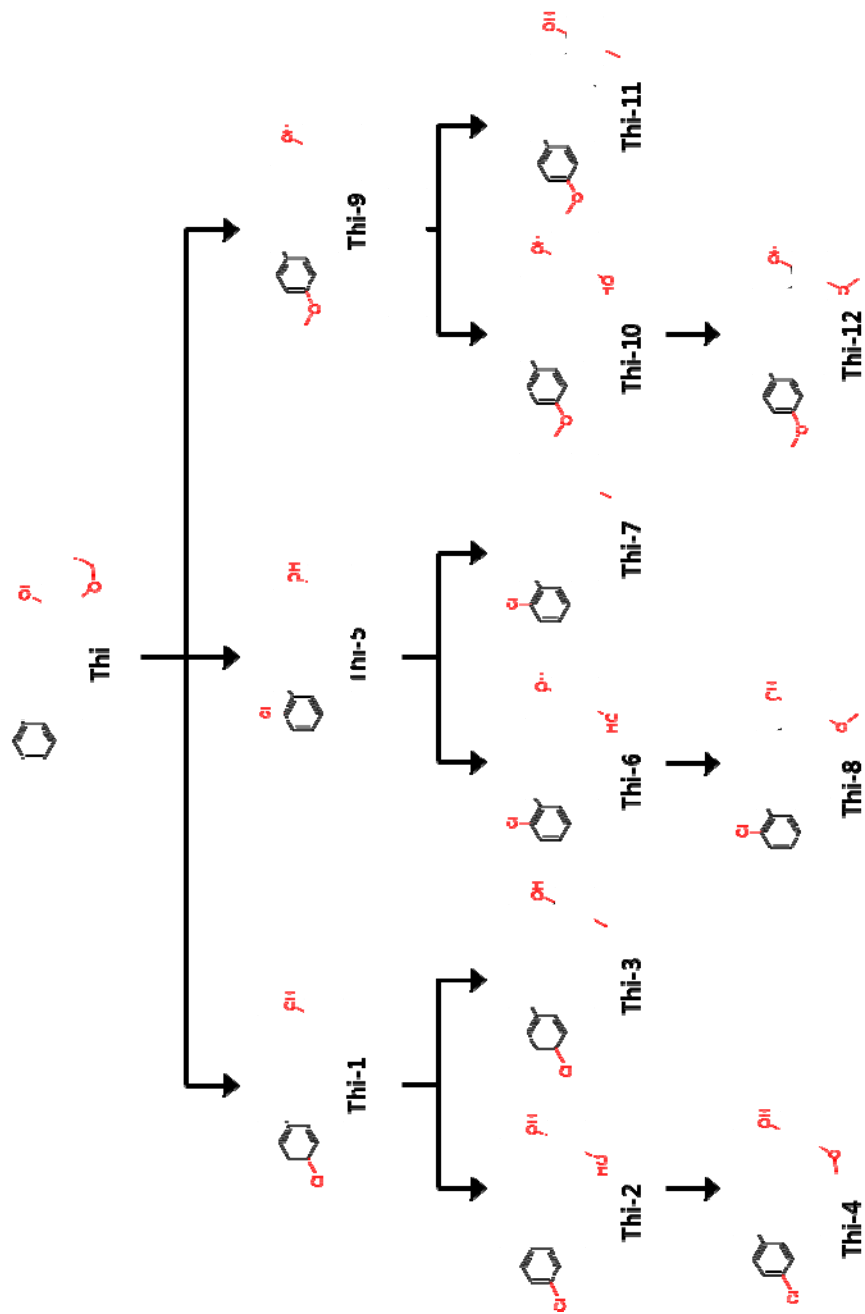
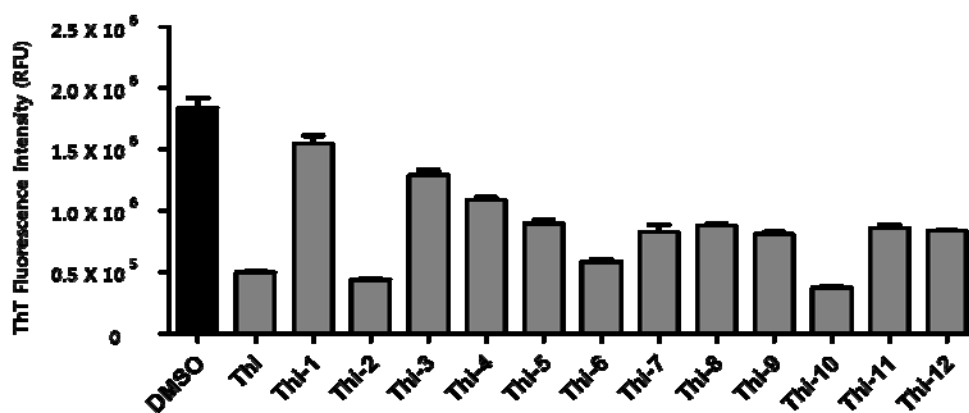


Figure 13. ThT fluorescence intensity of incubating Tau K18 with Thi analogs

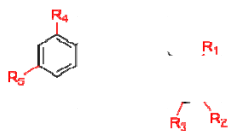
(A) To compare inhibition effects, Thi analogs (10 μ M) were incubated with Tau K18 (100 μ M) for 6 hours and Tau K18 aggregation was measured ThT fluorescence assay. Each independent experiment was performed in triplicate; data are expressed as means \pm S.D

(B) Measured fluorescence intensity was normalized by DMSO treated Tau K18

(A)



(B)



Compounds	R1 group	R2 group	R3 group	R4 group	R5 group	Aggregation (% of DMSO)
Thi	OH	$\begin{matrix} \text{CH}_3 \\ \\ \text{—O—CH}_2 \end{matrix}$	H	H	Cl	27.54 ± 0.50
Thi-1	OH	H	H	H	Cl	85.54 ± 4.06
Thi-2	OH	H	OH	H	Cl	24.06 ± 0.35
Thi-3	—OH	H	—CH ₃	H	—Cl	71.52 ± 2.32
Thi-4	—OH	H	—O—CH ₃	H	—Cl	60.24 ± 1.45
Thi-5	—OH	H	H	—Cl	H	48.54 ± 1.82
Thi-6	—OH	H	—OH	—Cl	H	32.30 ± 1.07
Thi-7	—OH	H	—CH ₃	—Cl	H	45.49 ± 3.70
Thi-8	—OH	H	—O—CH ₃	—Cl	H	45.85 ± 0.96
Thi-9	—OH	H	H	H	—O—CH ₃	44.60 ± 1.24
Thi-10	—OH	H	—OH	H	—O—CH ₃	20.53 ± 0.85
Thi-11	—OH	H	—CH ₃	H	—O—CH ₃	47.44 ± 1.61
Thi-12	—OH	H	—O—CH ₃	H	—O—CH ₃	46.24 ± 0.22

Figure 14. Synthesis scheme for thiazolidine (Thi) analogs

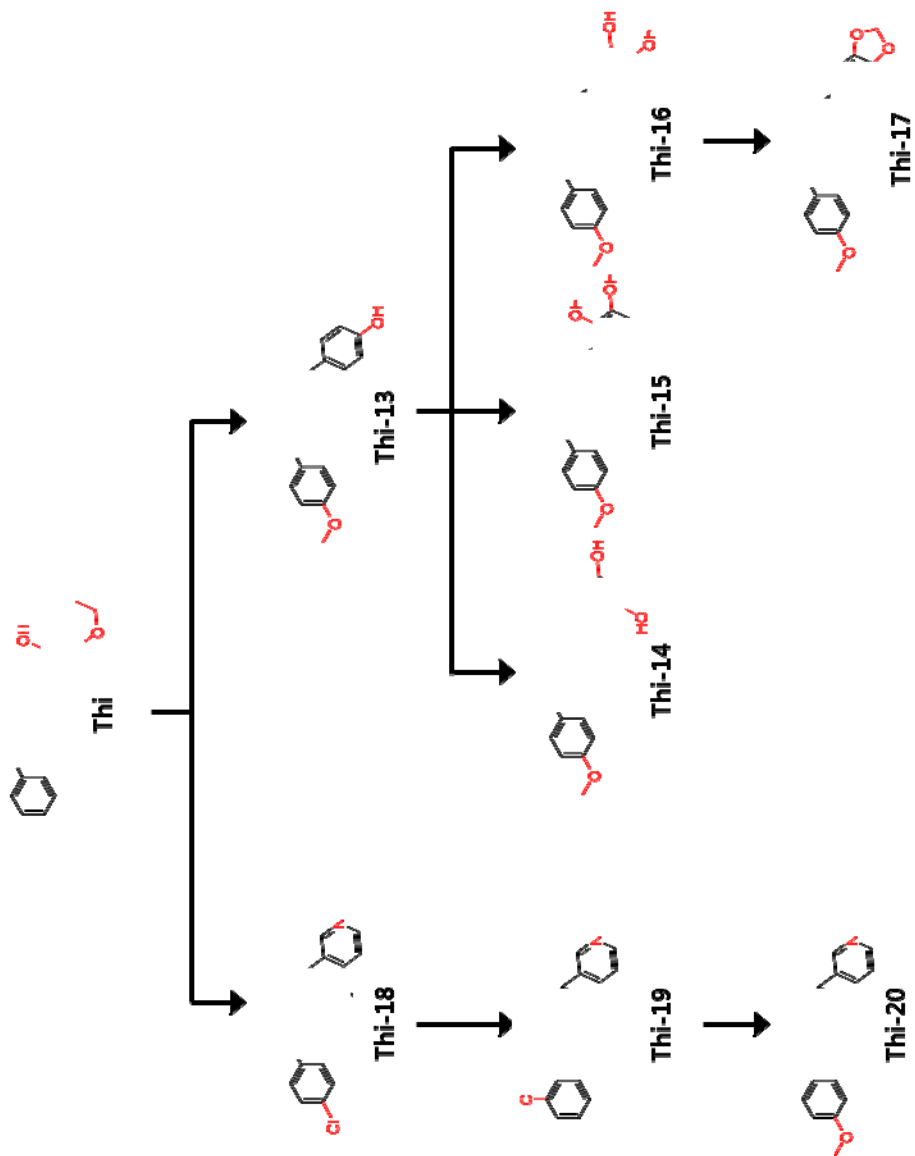
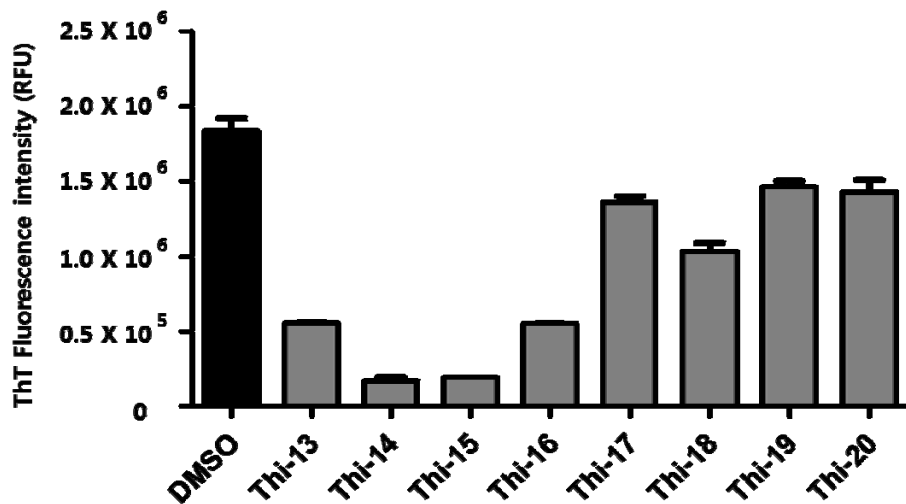


Figure 15. ThT fluorescence intensity of incubating Tau K18 with Thi analogs

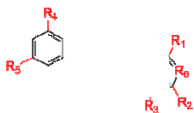
(A) To compare inhibition effects, thiazolidine (Thi) analogs (10 μ M) were incubated with Tau K18 (100 μ M) for 6 hours and Tau K18 aggregation was measured with ThT fluorescence assay. Each independent experiment was performed in triplicate; data are expressed as means \pm S.D

(B) Measured fluorescence intensity was normalized by DMSO treated Tau K18

(A)



(B)



Compounds	R1 group	R2 group	R3 group	R4 group	R5 group	R6 group	R7 group	Aggregation (% of DMSO)
Thi-13	H	H	-OH	H	H	-O-CH ₃	C	30.27 ± 0.48
Thi-14	H	-OH	-OH	H	H	-O-CH ₃	C	9.30 ± 1.81
Thi-15	-OH	-OH	H	H	H	-O-CH ₃	C	10.50 ± 0.33
Thi-16	-OH	H	H	-OH	H	-O-CH ₃	C	30.23 ± 0.23
Thi-17	-O-CH ₃	-O-CH ₃	H	-Cl	-O-CH ₃	-O-CH ₃	C	73.93 ± 2.38
Thi-18	H	H	H	H	H	-Cl	N	56.43 ± 3.09
Thi-19	H	H	H	H	-Cl	H	N	79.68 ± 2.29
Thi-20	H	H	H	H	H	-O-CH ₃	N	77.73 ± 4.49

Figure 16. Dose-dependent inhibition by thiazolidine (Thi) analogs

Tau K18 (100 μ M) were incubated with various concentration of Thi analogs (0.01, 0.1, 1, 10 and 100 μ M) and inhibition effect was measured by ThT assay. Measured fluorescence intensity was normalized by DMSO treated Tau K18.

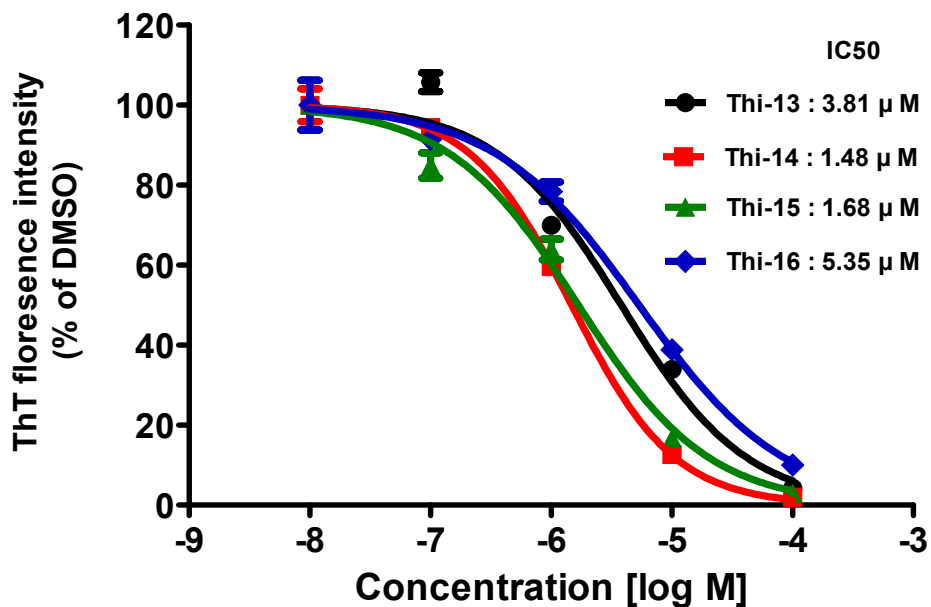
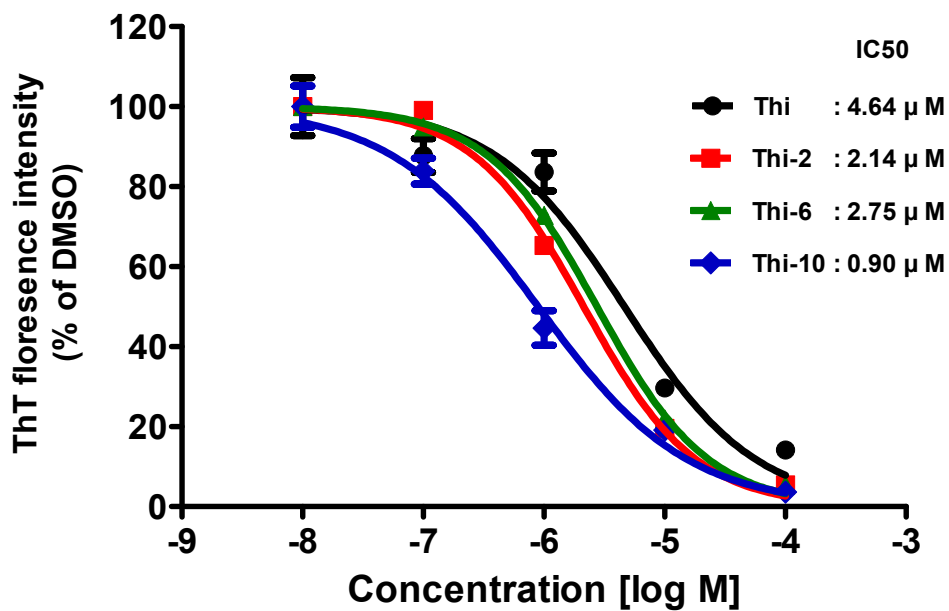


Figure 17. Synthesis scheme for dimethylphenazine (DMP) analogs

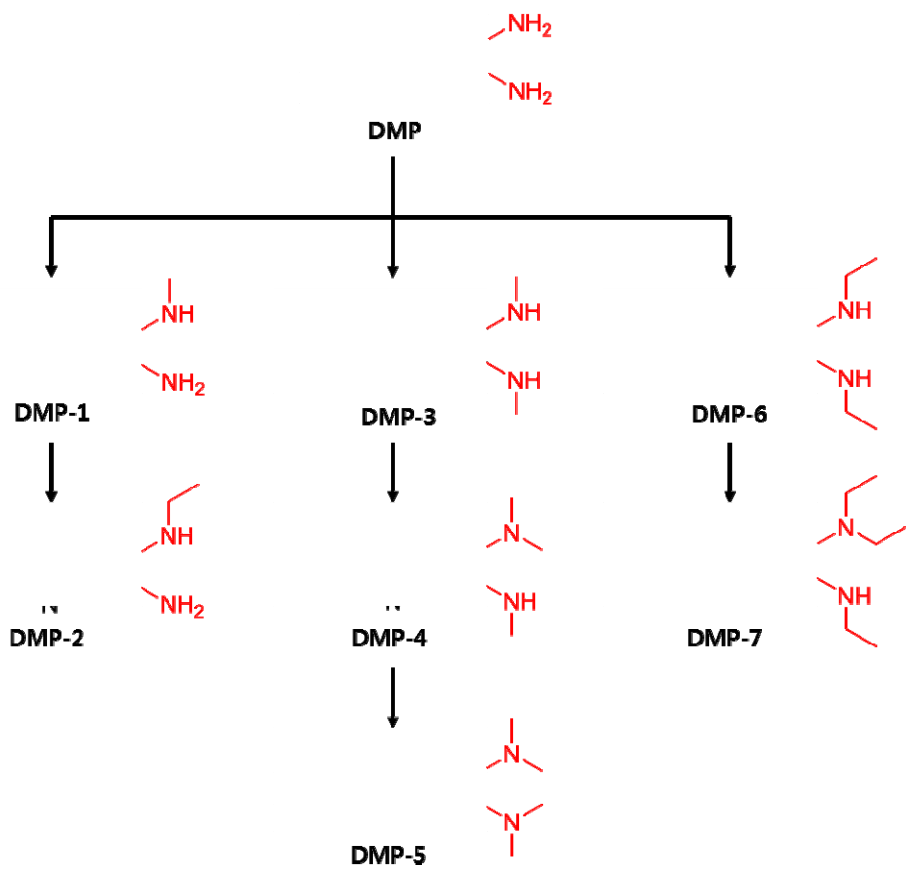
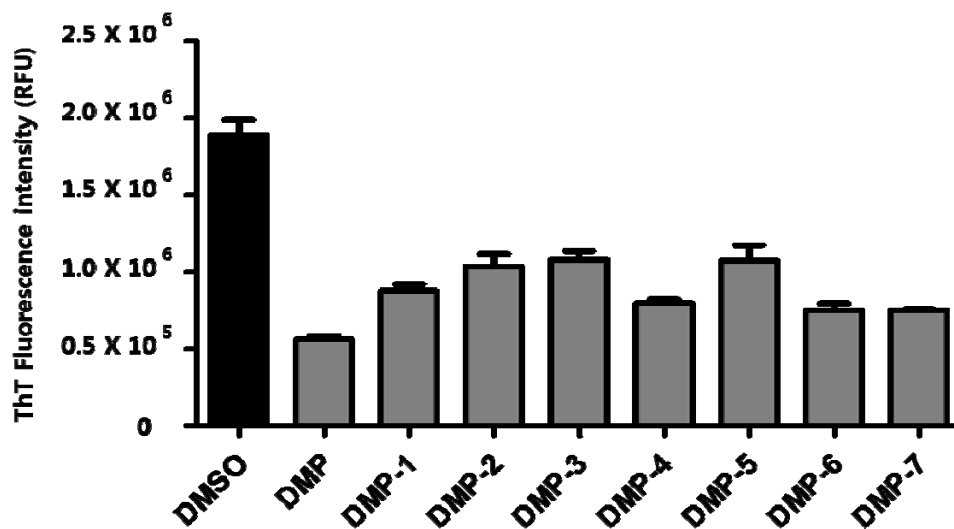


Figure 18. ThT fluorescence intensity of incubating Tau K18 with DMP analogs

(A) To compare inhibition effects, DMP analogs (10 μ M) were incubated with Tau K18 (100 μ M) for 6 hours and Tau K18 aggregation was measured by ThT fluorescence assay. Each independent experiment was performed in triplicate; data are expressed as means \pm S.D

(B) Measured fluorescence intensity was normalized by DMSO treated Tau K18

(A)



(B)

$-R_1$

$-R_2$

Compounds	DMP	DMP-1	DMP-2	DMP-3	DMP-4	DMP-5	DMP-6	DMP-7
R1 group	$-\text{NH}_2$	$-\text{N}(\text{CH}_3)_2$	$-\text{N}(\text{CH}_3)(\text{CH}_2)$	$-\text{N}(\text{CH}_3)_2$	$-\text{N}(\text{CH}_3)_2$	$-\text{N}(\text{CH}_3)_2$	$-\text{N}(\text{CH}_3)(\text{CH}_2)$	$-\text{N}(\text{CH}_3)_2$
R2 group	$-\text{NH}_2$	$-\text{NH}_2$	$-\text{NH}_2$	$-\text{N}(\text{CH}_3)_2$	$-\text{N}(\text{CH}_3)_2$	$-\text{N}(\text{CH}_3)_2$	$-\text{N}(\text{CH}_3)(\text{CH}_2)$	$-\text{N}(\text{CH}_3)(\text{CH}_2)$
Aggregation (% of DMSO)	29.57 ± 1.38	46.33 ± 2.37	54.86 ± 4.24	56.93 ± 3.31	42.09 ± 1.39	56.71 ± 5.46	39.73 ± 2.34	36.69 ± 0.34

Figure 19. Dose-dependent inhibition by DMP analog

Tau K18 (100 μ M) were incubated with various concentration of DMP analogs (0.01, 0.1, 1, 10 and 100 μ M) and inhibition effect was measured by ThT assay. Measured fluorescence intensity was normalized by DMSO treated Tau K18.

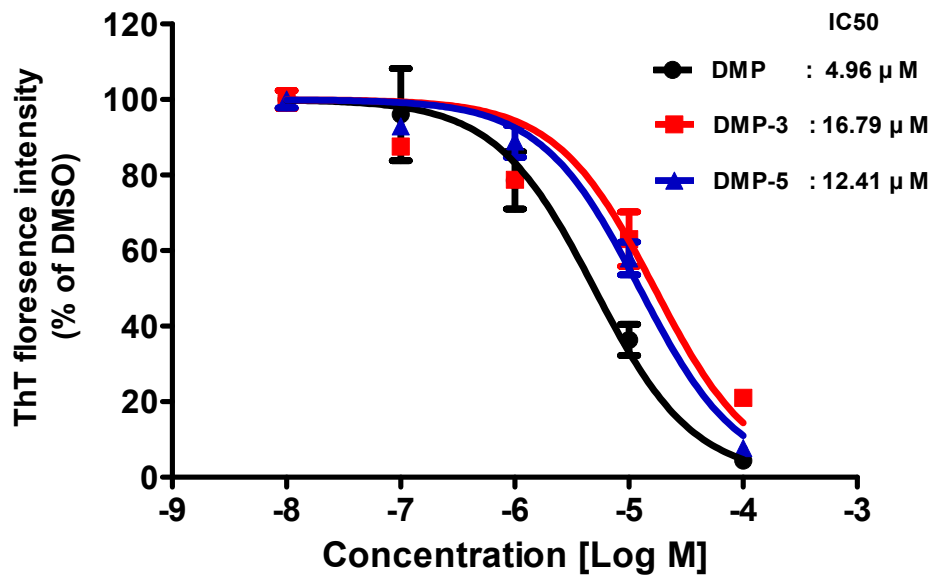
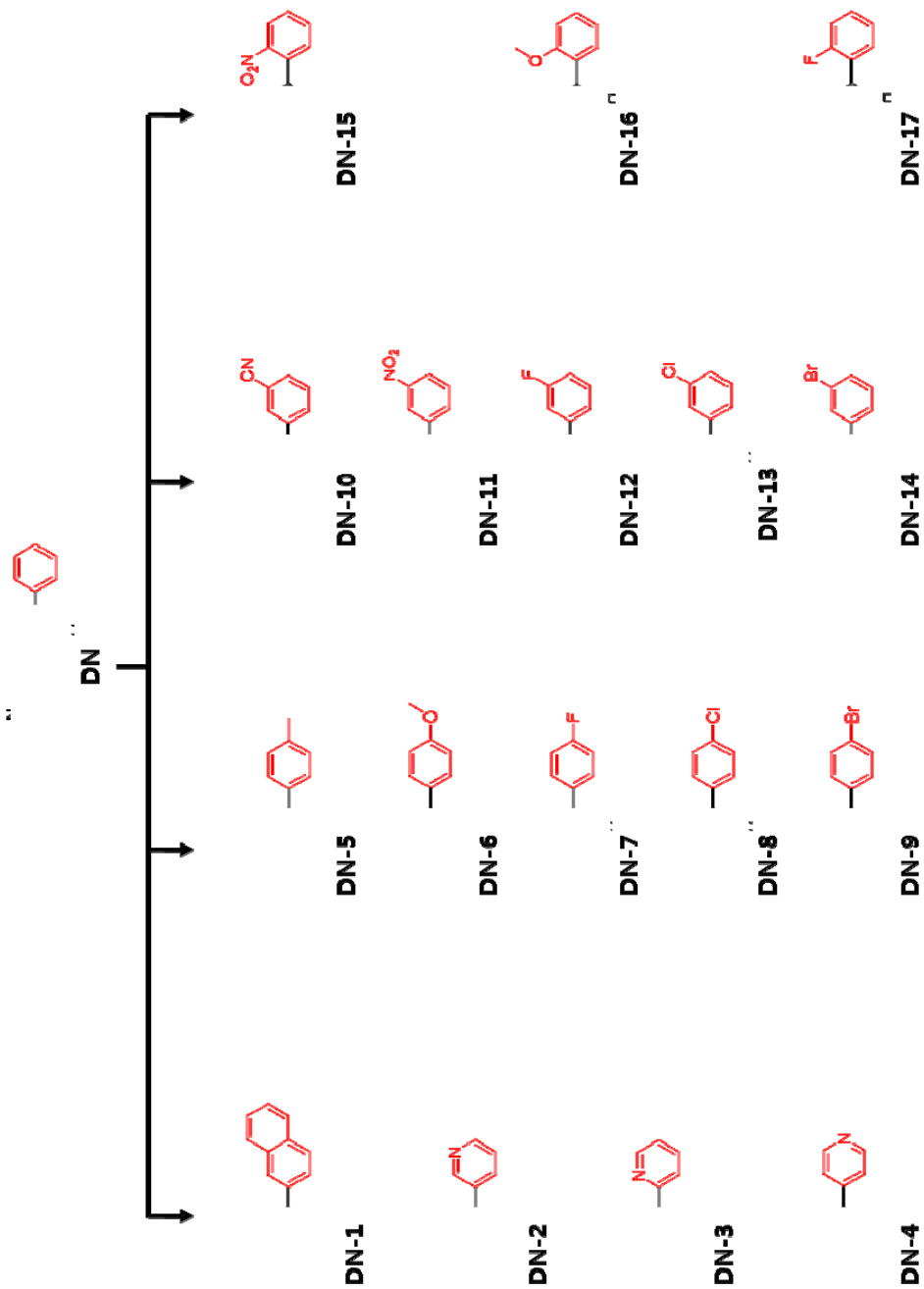


Figure 20. Synthesis scheme for *De novo* (DN) scaffold analogs

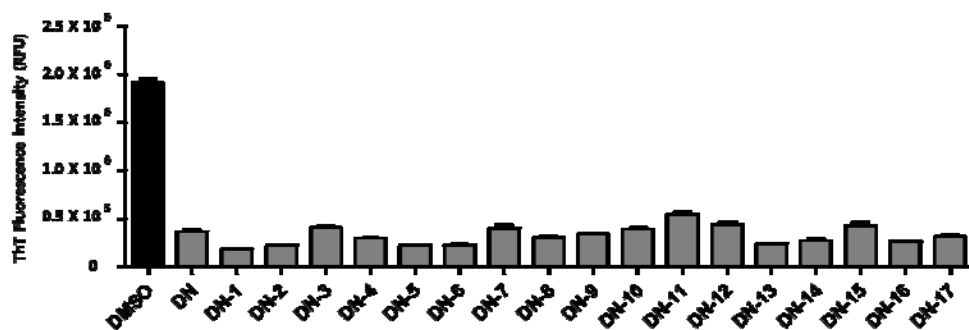


**Figure 21. ThT fluorescence intensity of incubating Tau K18 with
DN analogs**

(A) To compare inhibition effects, DN analogs (10 μ M) were incubated with Tau K18 (100 μ M) for 6 hours and Tau K18 aggregation was measured by ThT fluorescence assay. Each independent experiment was performed in triplicate; data are expressed as means \pm S.D

(B) Measured fluorescence intensity was normalized by DMSO treated Tau K18

(A)



(B)

-R

Compounds	DN	DN-1	DN-2	DN-3	DN-4	DN-5	DN-6	DN-7	DN-8
R group									
Aggregation (% of DMSO)	29.57 ± 1.58	46.33 ± 2.37	54.86 ± 4.24	56.89 ± 3.31	42.09 ± 1.39	56.71 ± 5.46	38.73 ± 2.34	38.69 ± 0.34	38.69 ± 0.34

Compounds	DN-9	DN-10	DN-11	DN-12	DN-13	DN-14	DN-15	DN-16	DN-17
R group									
Aggregation (% of DMSO)	29.57 ± 1.58	46.33 ± 2.37	54.86 ± 4.24	56.89 ± 3.31	42.09 ± 1.39	56.71 ± 5.46	38.73 ± 2.34	38.69 ± 0.34	38.69 ± 0.34

Figure 22. Dose-dependent inhibition by DN analog

Tau K18 (100 μ M) were incubated with various concentration of DN analogs (0.01, 0.1, 1, 10 and 100 μ M) and inhibition effect was measured by ThT fluorescence assay. Measured fluorescence intensity was normalized by DMSO treated Tau K18.

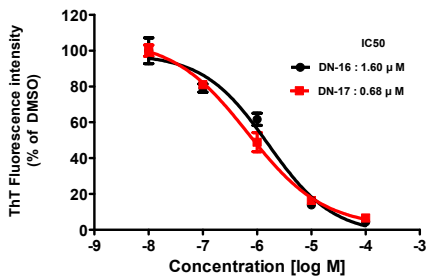
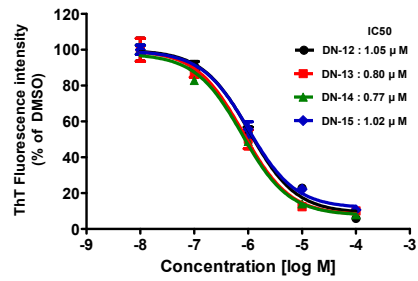
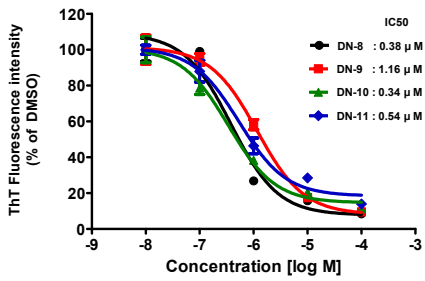
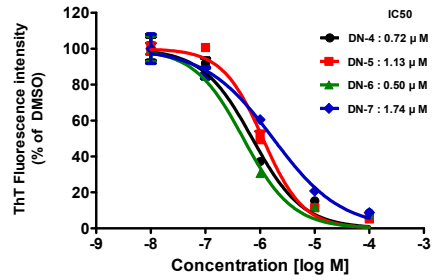
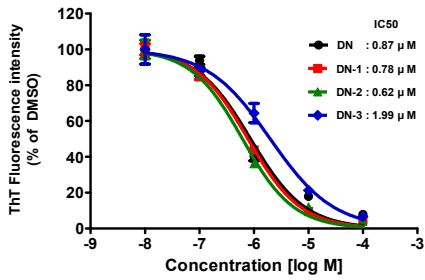
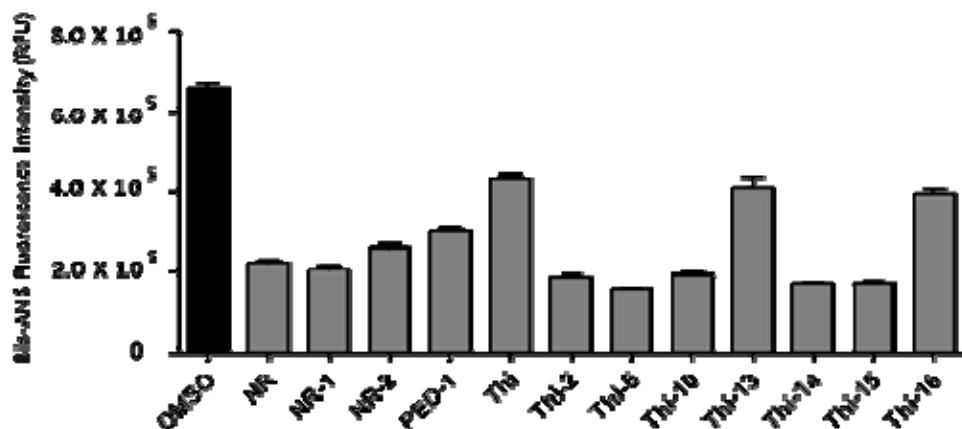


Figure 23. Bis-ANS fluorescence intensity of incubating Tau K18 with NR, PED, Thi analogs

(A) Analogs (10 μ M) were incubated with Tau K18 (100 μ M) for 6 hours and surface hydrophobicity was measured by Bis-ANS fluorescence assay. Each independent experiment was performed in triplicate; data are expressed as means \pm S.D

(B) Measured fluorescence intensity was normalized by DMSO treated Tau K18

(A)



(B)

(DMSO : 100%)

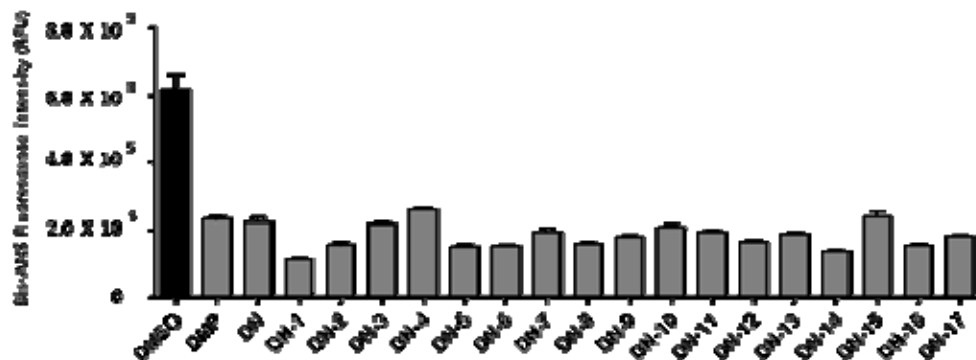
Compounds	NR	NR-1	NR-2	PED-1	Thi	Thi-2
Normalized fluorescence	34.18 ± 0.59	31.32 ± 1.48	39.73 ± 1.62	46.19 ± 1.16	66.40 ± 1.27	28.81 ± 0.72
Compounds	Thi-6	Thi-10	Thi-13	Thi-14	Thi-15	Thi-16
Normalized fluorescence	24.10 ± 0.26	29.67 ± 1.14	62.53 ± 4.59	26.14 ± 0.56	26.38 ± 0.73	60.57 ± 1.95

Figure 24. Bis-ANS fluorescence intensity of incubating Tau K18 with DN analogs

(A) Analogs (10 μ M) were incubated with Tau K18 (100 μ M) for 6 hours and surface hydrophobicity was measured by Bis-ANS fluorescence assay. Each independent experiment was performed in triplicate; data are expressed as means \pm S.D

(B) Measured fluorescence intensity was normalized by DMSO treated Tau K18

(A)



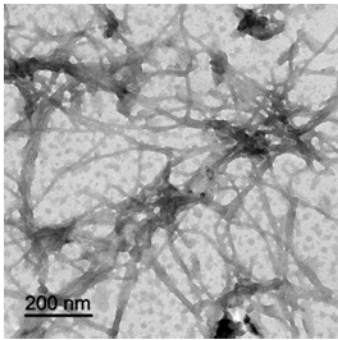
(B)

(DMSO : 100%)

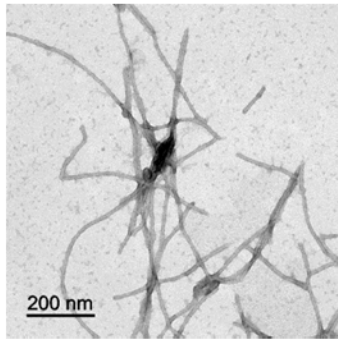
Compounds	DMP	DN	DN-1	DN-2	DN-3	DN-4	DN-5
Normalized fluorescence	34.18 ± 0.59	31.32 ± 1.48	39.73 ± 1.62	46.19 ± 1.16	66.40 ± 1.27	28.81 ± 0.72	28.81 ± 0.72
Compounds	DN-6	DN-7	DN-8	DN-9	DN-10	DN-11	DN-12
Normalized fluorescence	24.10 ± 0.26	29.67 ± 1.14	62.53 ± 4.59	26.14 ± 0.56	26.38 ± 0.73	60.57 ± 1.95	60.57 ± 1.95
Compounds	DN-13	DN-14	DN-15	DN-16	DN-17		
Normalized fluorescence	24.10 ± 0.26	29.67 ± 1.14	62.53 ± 4.59	26.14 ± 0.56	26.38 ± 0.73		

Figure 25. Observing Tau aggregates with analogs by TEM

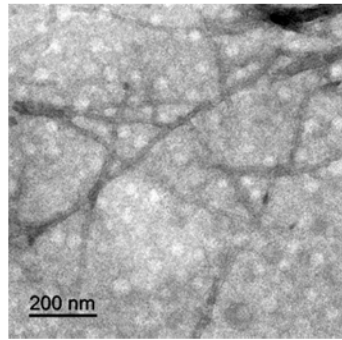
Tau K18 aggregates (100uM) with DMSO or analogs (10uM) were incubated 37°C for 24 hours and stained with 1% uranyl acetate.



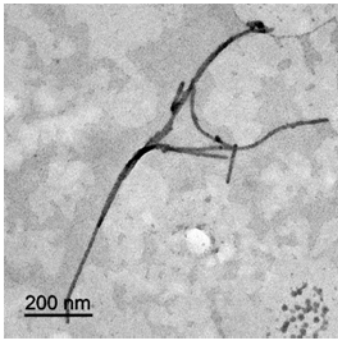
DMSO



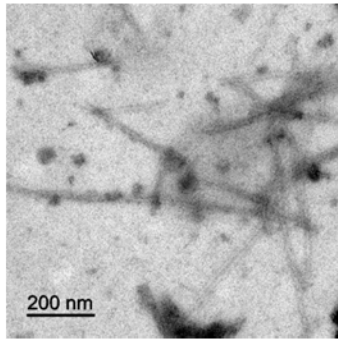
NR



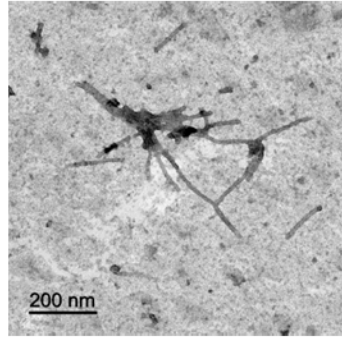
NR-1



NR-2



PED-1

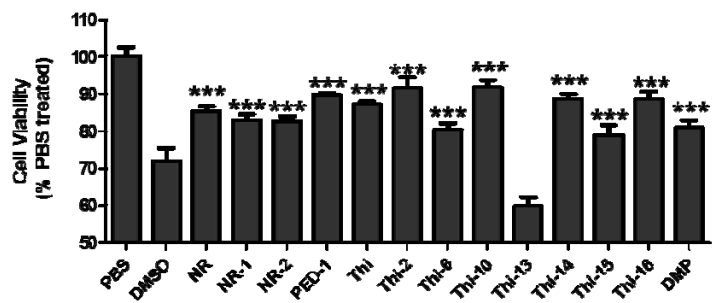


DMP

Figure 26. Reducing cytotoxicity of Tau K18 aggregates by analogs

Tau K18 (100 μ M) was aggregated with DMSO or analogs (100 μ M) and these aggregates treated to SH-SY5Y cells at a ratio of 1:1000. After 24 hours, cell viability was measured by using MTT assay and normalized by PBS only. *Statistically significant difference ($P < 0.05$ by Dunnett's test) compared with DMSO control group (n = 6)

(A)



(B)

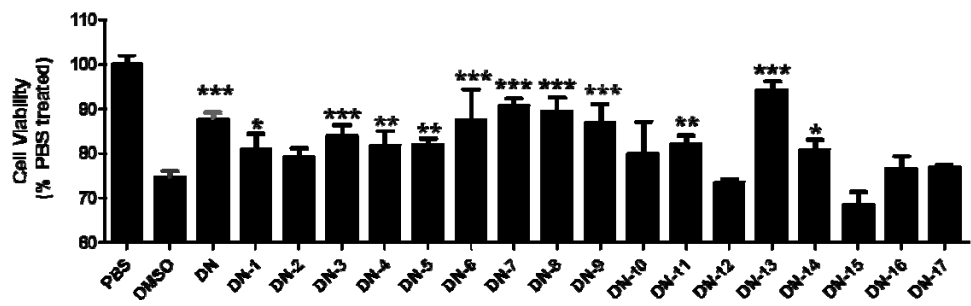


Figure 27. Dose-dependent disruption aggregates by analogs

Tau K18 (100 μ M) were aggregated for 6 hours and various concentration analogs (0.01, 0.1, 1, 10 and 100 μ M) were treated to aggregated Tau K18. Disruption effect was measured by ThT fluorescence assay. Measured fluorescence intensity was normalized by DMSO treated Tau K18. DC50 concentrations were re-assessed for aggregation line using dose-response curves generated by GraphPad Prism software

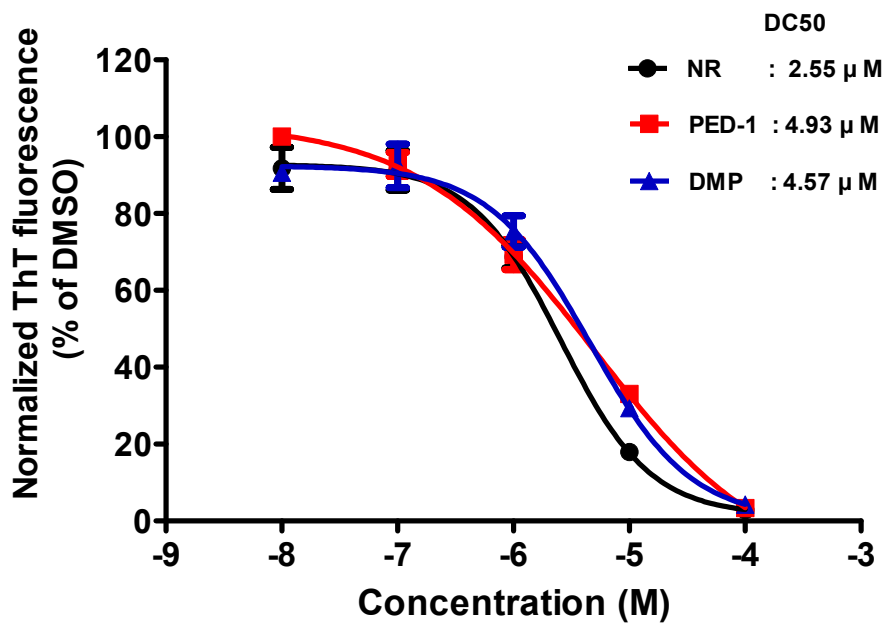


Figure 28. Time course of inhibition by NR, PED, DMP and Thi analogs

Tau K18 aggregation were measured by ThT fluorescence intensity every 2 hours for 12 hours at low concentration of analogs (5 μ M).

Each independent experiment was performed in triplicate and normalized by 8 hours DMSO treated Tau K18; data are expressed as means \pm S.D.

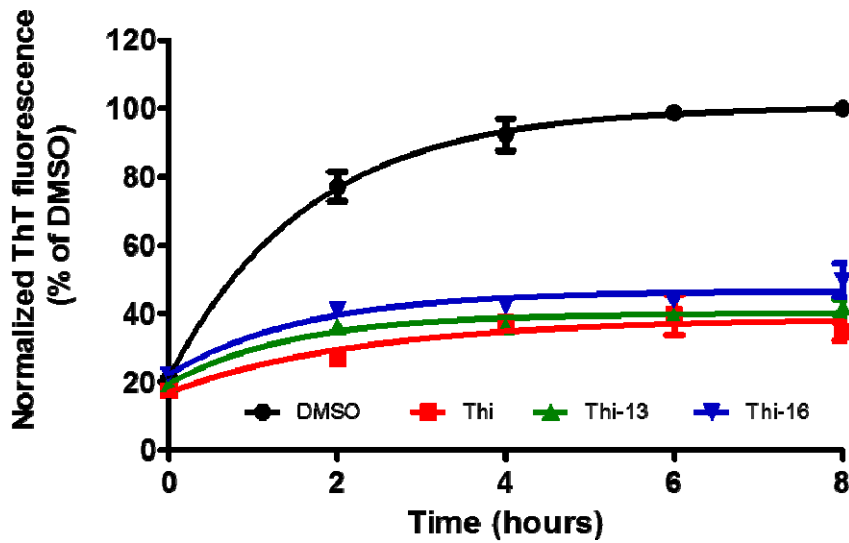
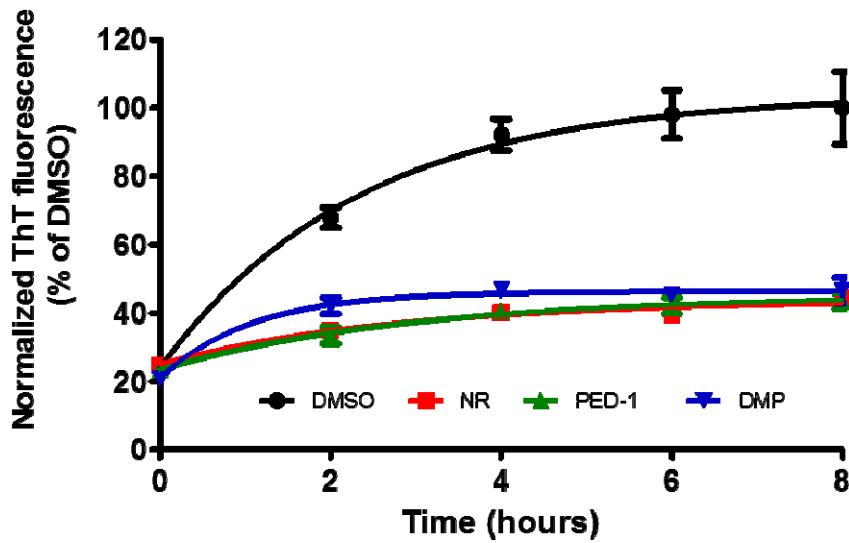


Figure 29. Time course of inhibition by DN analogs

Tau K18 aggregation were measured by ThT fluorescence intensity every 2 hours for 12 hours in low concentration of analogs (1 μ M).

Each independent experiment was performed in triplicate and normalized by 8 hours DMSO treated Tau K18; data are expressed as means \pm S.D.

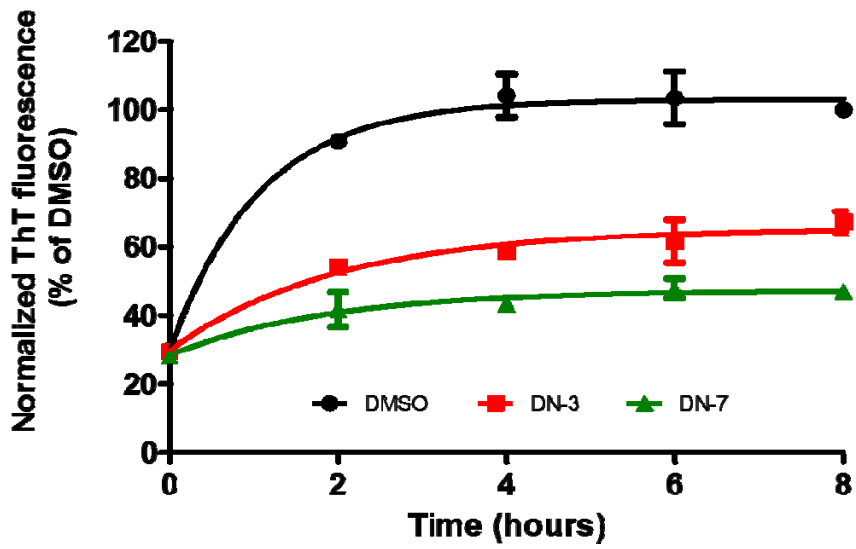


Figure 30. Time course of disruption by NR, PED, DMP and Thi analogs

Tau K18 that had been aggregated for 6 hours to make pre-aggregates and analogs (5 μM) was treated to pre-aggregated Tau K18 (100 μM). Disruption by analogs was measured by ThT fluorescence intensity for 0, 5, 30, and 60 min. Each independent experiment was performed in triplicate and normalized by DMSO-treated Tau K18; data are expressed as means \pm S.D.

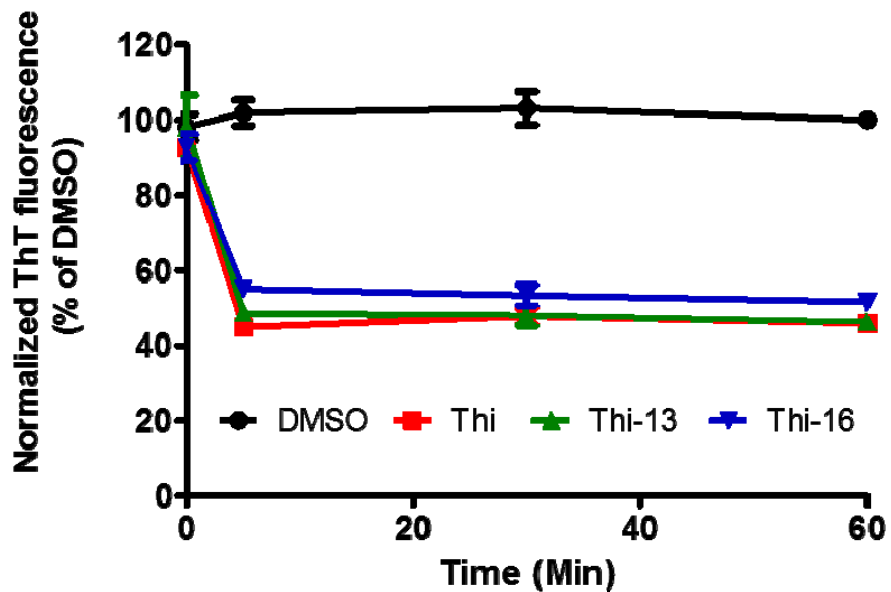
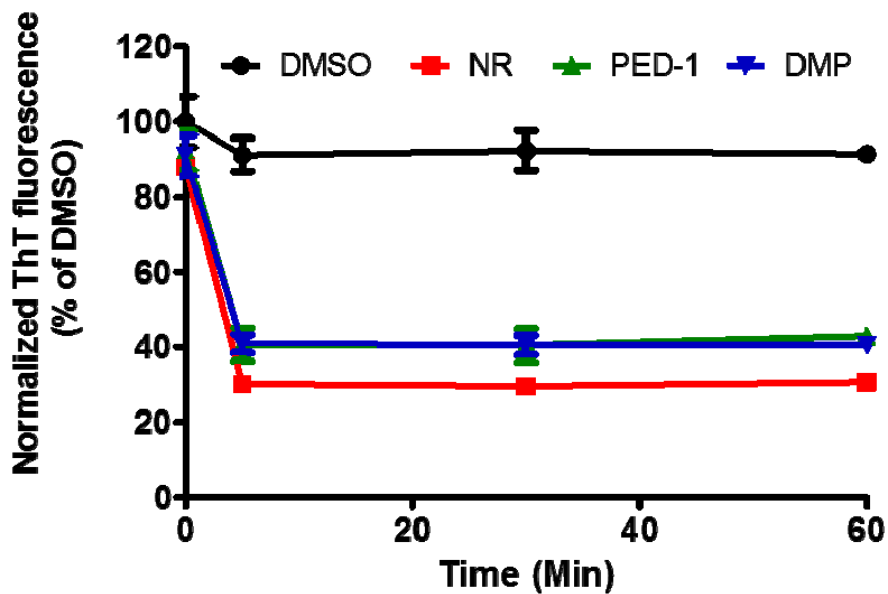


Figure 31. Time course of disruption by DN analogs

Tau K18 that had been aggregated for 6 hours to make pre-aggregates and analogs (1 μM) was treated to pre-aggregated Tau K18 (100 μM). Disruption by analogs was measured by ThT fluorescence intensity for 0, 5, 30, and 60 min. Each independent experiment was performed in triplicate and normalized by DMSO-treated Tau K18; data are expressed as means \pm S.D.

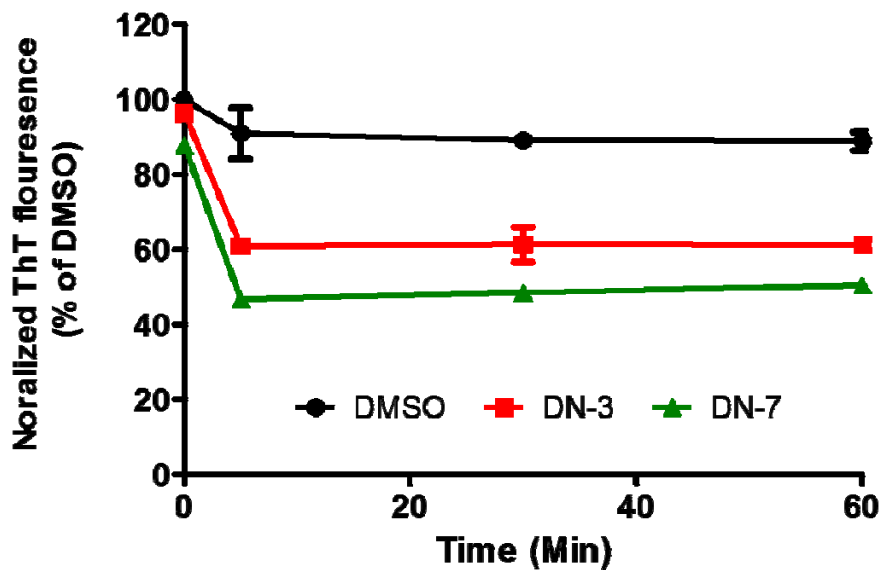
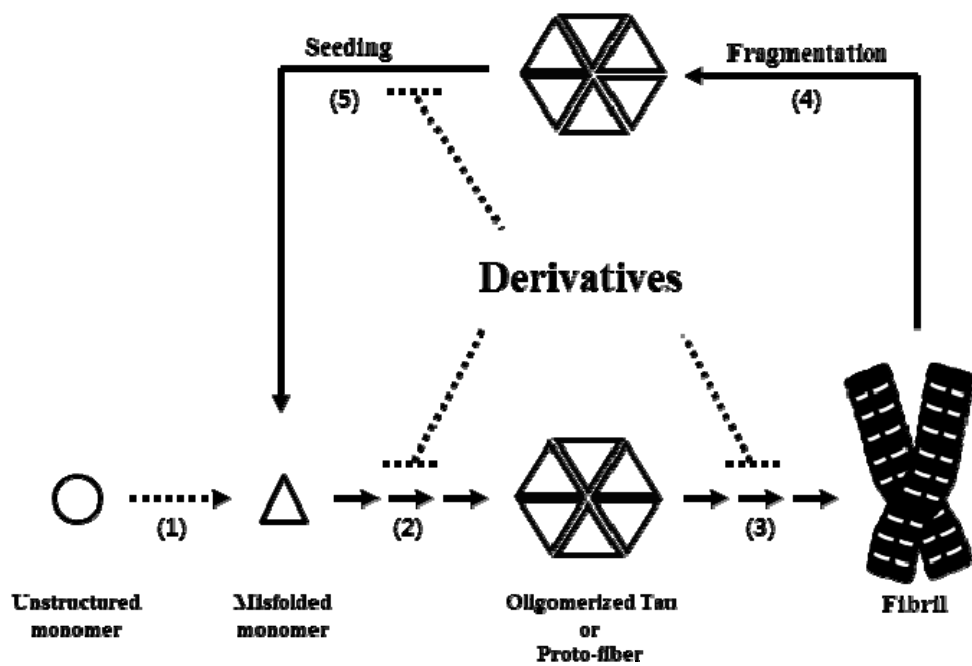


Figure 32. Working model of analogs on Tau K18 aggregation

Step 1 to step 3 represent the primary aggregation pathway, including misfolded pathway (step 1), oligomerized pathway (step 2), and fiberization pathway (step 3). Step 4 to Step 5 showed fibril-catalyzed secondary aggregation pathway. Analogs acted on improperly folded Tau and inhibited oligomerization (stage 2), rather than suppressing miss-folding process (step 1). Also, analogs acted on oligomerized or proto-fiber Tau, inhibiting fiberization (step 3), and disrupted Tau seeds which could promote aggregation (step 5).



DISCUSSION

Tau aggregates can propagate by an autocatalytic mechanism such as prion-like replication. This replication is considered the major process for spreading Tau aggregates in cellular tissue^{2, 32-33}. Therefore, it is important for a therapeutic agent to inhibit or reduce aggregates. In the present study, we performed screening based on ThT fluorescence assays to determine compounds that inhibit Tau aggregation and screened eight novel compounds (Figure 4). For analog synthesis, four compounds (NR, PED, DMP, and Thi) were selected as the scaffold and a DN compound was designed based on screening results (Figure 5). A total of 57 analogs were synthesized and their inhibitory effects on Tau K18 aggregation based on scaffolds and modified residues were characterized. NR, PED, and DMP were scaffolds with restrictions whose inhibitory effects decreased as the size of the modified residue increased (Figures 7, 10, and 18). However, the Thi scaffold inhibited Tau K18 aggregation more efficiently as hydroxyl groups increased (Figures 13 and 15). The number of hydroxy groups was an important variable for the inhibitory effect; however, some sites also had increased cytotoxicity (Figure 26). Finally, all of the analogs synthesized based on the DN compound showed excellent inhibitory

effects (Figure 21); however, the toxicity of Tau K18 aggregates was reduced to a similar degree as that of other scaffold-based analogs (Figure 26). This difference was presumed to be caused by higher compound cytotoxicity of DN analogs than that of other analogs. Therefore, DN analogs presented limitations in that they reduced the compound cytotoxicity of analogs.

Tau K18 aggregation is a very complex process involving the sequential formation of various Tau aggregates, including oligomers, proto-fibers, and fibrils. Previous studies have stated that Tau aggregation occurs via a lag phase, elongation phase, and saturation phase^{30, 34}. During the lag phase, Tau monomers are altered from a random coil into a solvent exposed hydrophobic β -sheet-rich structure. Then, during the elongation phase, the misfolded Tau forms proto-fibrils through the oligomer by self-assembly and proto-fibrils maturing into fibrils during the saturation phase. In addition, oligomers and proto-fibrils act as seeds for inducing misfolding and aggregation of Tau. IC50 and DC50 values predicted that analogs would inhibit aggregation and disrupt aggregates via a similar process (Figures 8, 11, 19, and 27). This prediction has been confirmed in other aggregation inhibitors in previous studies. Inhibitors such as brazilin³⁵, resveratrol²⁶, and epigallocatechin gallate (EGCG)³⁶⁻³⁷ induce structural changes

in Tau aggregates and inhibit aggregation. Tau K18 aggregation with analogs rapidly increased from 0 hour to 4 hours without a lag phase (Figures 29 and 30). This tendency indicated that analogs did not affect the lag phase and initial elongation phase, and that Tau K18 aggregates with analogs were instantly decreased below 50% compared to DMSO and remained constant (Figures 31 and 32). From these results, it is expected that analogs could not inhibit misfolding by inducer and low n-oligomerization. However, we predicted that the Tau aggregation that was inhibited by inducing structural changes at a certain level of Tau aggregates can serve as seeds (Figure 33).

Finally, in ThT-based screening, we showed that inhibitors such as resveratrol and EGCG were more likely to be screened than compounds that inhibit misfolding or block Tau-Tau interactions.

Chapter 2

Measurement of membrane
binding in Tau aggregates using
fluorescence

INTRODUCTION

Soluble and unstructured protein Tau binds to microtubules in the central nervous system to stabilize and promote their assembly ⁶. However, under pathological conditions, Tau dissociates from microtubules and aggregates into neurofibrillary tangles ⁴⁻⁵. Aberrant aggregation and deposition of Tau is one of the major causes of several neurodegenerative diseases including Alzheimer's disease (AD), Parkinson's disease, and frontal temporal dementia linked to chromosomes ^{1, 38-39}. Accumulation evidence has shown that Tau aggregates are not only cytotoxic, but also propagate in neurons ^{2, 24, 40}. Tau propagation, such as prion-like propagation, is recognized as an important pathogenesis mechanism of Tau-related diseases in the brain. Tau propagation has been demonstrated by injecting brain lysates from late-stage disease mice into young AD model mice ³². When injected into the hippocampus and cerebral cortex, brain lysate extracts induced Tau pathology in non-symptomatic young AD model mice and Tau aggregates spread from the injection site to synaptic connected areas. In addition, synthetic fibrils can also induce native Tau into forming pathological aggregates in transgenic mice ¹² and cultured cells ^{11, 41-42}.

However, the mechanism behind Tau propagation has not been elucidated to date. Recently, endocytosis or micropinocytosis through the cell membrane has been predicted as playing an important role in Tau propagation⁴³⁻⁴⁴. When membrane binding is inhibited by neutralizing the Tau aggregates through antibodies, Tau propagation is inhibited⁴⁵⁻⁴⁶. In the present study, we focused on developing a measuring method for membrane binding of Tau aggregates. To measure membrane binding of Tau that was dependent on aggregation, Tau was fluorescently labeled. This allowed the measurement of membrane binding in living cells. Various Tau aggregates were prepared and membrane binding was compared by fluorescence measurement.

MATERIALS AND METHODS

Purification and labeling of recombinant Tau K18

A Tau K18 fragment (containing the microtubule-binding domain) was subcloned into pET-16b for tagging N-terminal 6xHis. Constructed plasmid was transformed into BL21(DE3)/RIL. Transformants were grown in LB media at 37°C until OD₆₀₀ reached 0.8. Expression of recombinant Tau K18 was induced with 1 mM IPTG and further incubated for 2 h at 37°C. Then, cells were harvested by centrifugation at 4,000 × g for 15 min and re-suspended in PBS buffer (5 mM DTT and 1 mM PMSF). Re-suspended cell pellets were sonicated and centrifuged at 16,000 × g for 15 min. Cleared lysate was passed through Ni Sepharose 6 Fast Flow resin (GE healthcare) and bound protein was eluted with 250 mM imidazole. Finally, purified protein was dialyzed using a Snakeskin dialysis tube (ThermoFisher) overnight against PBS buffer at 4°C under constant stirring to remove imidazole and degrade the fragment. The purified recombinant Tau K18 concentration was determined by OD₂₈₀ using an extinction coefficient of 4,080 M⁻¹cm⁻¹. Purified Tau K18 was conjugated to a Flamma 496 NHS ester (Bioact) in PBS buffer following the manufacturer's instructions. Excess dye was removed with a Snakeskin dialysis tube (Thermofisher). The labeling concentration was 2.7 mol dye per mole

of protein for recombinant Tau K18.

***In vitro* Tau K18 aggregation**

Recombinant Tau K18 containing 20% labeled Tau K18 (100 μ M) was incubated with agitation in PBS buffer (2 mM DTT) for up to 6 h in the presence of aggregation inducer ODS (50 μ M). After incubation, reactions were immediately subjected to SDS-PAGE analysis, ThT fluorescence assay, or membrane binding assay as described below.

SDS-PAGE analysis

To separate soluble from insoluble Tau K18, samples were centrifuged at $16,000 \times g$ for 15 min. Pellets were re-suspended in PBS buffer. The supernatant and re-suspended pellets were boiled for 10 min in the presence of the sample buffer, then applied to 15% polyacrylamide gels. Following SDS-PAGE analysis, Tau K18 was visualized by Coomassie blue staining and imaged by a luminograph II (ATTO). Additionally, trypsinized Tau K18 was visualized by processing as previously described.

Thioflavin T (ThT) fluorescence assay

ThT was dissolved in PBS buffer to 1 mM and stored at 4°C. A total of 50 μ M ThT was added to the aggregated sample and fluorescence

was measured in triplicate in white 96-well plates (31296, SPL) using a multilabel plate reader (EnVisoin, Perkin Elmer) at excitation and emission wavelengths of 440 and 485 nm, respectively.

Cell culture

HT22, SH-SY5Y, B103, and HEK293T cells were cultured in DMEM supplemented with 10% FBS and 1% antibiotics/antimycotic solution. Cells were maintained in a 5% CO₂ humidified atmosphere at 37°C and grown until 80% confluence.

Membrane binding analysis

HT22, SH-SY5Y, B103, and HEK293T cells were treated with 0.25% trypsin for 3 min and re-suspended in PBS buffer. Aggregated Tau K18 was treated for up to 1 h at 4°C in 300,000 cells and unbound Tau K18 was washed twice with cold PBS buffer solution. Treated cells were counted in a flow cytometer (FACSCanto, BD bioscience), each experiment was conducted three times, and 20,000 cells were counted in each individual experiment. To remove membrane bound Tau K18, Tau cells were treated with 0.125% trypsin for 3 min at 37°C and washed twice with PBS buffer solution.

RESULTS

Aggregation with fluorescence labeled Tau K18

We used a mixture containing 20% labeled Tau K18 and 80% unlabeled Tau K18 in all experiments to minimize possible interference with the fluorescence label. This mixture was incubated with ODS inducer to obtain aggregation⁴⁷⁻⁴⁸. To validate aggregation of this mixture, aggregation kinetics were measured by ThT fluorescence assay and SDS-PAGE analysis. ThT fluorescence assay analysis represented the formation of the β -sheet structure during aggregation that is one of the key features of amyloid proteins⁴⁹⁻⁵⁰. Unlabeled Tau K18 showed an exponential phase after a 1-h lag phase and a stationary phase after 4 h. This tendency was also observed in the aggregation mixture containing labeled Tau K18 (Figure 33). Additionally, it was found that the amount of insoluble aggregates in the mixture increased over time (Figure 34). These results show that the 20% fluorescence labeled Tau K18 did not interfere with the aggregation of Tau K18.

Membrane binding of Tau K18 aggregates

To measure binding, cells were treated with Tau K18 aggregates at low temperature (4°C) over various times (0, 15, 30, 45, and 60 min),

and cells containing Tau K18 were analyzed with a FACSCanto. Low temperature incubation was an important process for observing membrane binding because the transport pathway is inhibited at low temperatures^{44, 51}. A significant amount of Tau K18 aggregates were found to bind to cells within a relatively short time (15 min) and the binding of Tau K18 continuously increased until 60 min (Figure 35A, B). Additionally, membrane binding of Tau K18 aggregates was not significantly different in PBS or DMEM (with 10% FBS) (Figure 36A, B). Next, Tau K18 bound to membranes was removed with trypsin to confirm Tau K18 uptake. Tau K18 on cell membranes was reduced by more than 50%, but still 20% remained (Figure 37A, B). This remaining 20% was less degraded Tau K18 than cellular uptake (Figure 38). In the presence of Tau K18 alone, 3 min was a sufficient time for complete degradation (Figure 39). However, complete degradation was difficult because membrane proteins of cells act as competitors for the degradation of Tau K18. Tau K18 aggregates become bound to cell membranes within 1 h at low temperatures and they were not taken up by cells.

Aggregation-dependent membrane binding of Tau K18

Aggregated Tau was more easily taken up by cells than monomer Tau^{43, 52}. This tendency was also observed in membrane binding. Various Tau K18 aggregates were generated over different times (0, 2, 4, and 6 h) and aggregates were presented to cells. After aggregating for 2 h, a significant amount of Tau K18 was bound to membranes and, as aggregation progressed, the amount of membrane bound Tau K18 increased (Figure 40A, B). Next, to investigate the dynamic range of membrane binding, several concentrations (0.5, 1, 5, and 10 μM) of Tau K18 aggregates were presented to cells. Tau K18 bound to membranes in a dose-dependent manner (Figure 41A, B). At 0.5 and 0.1 μM , less than 20% of Tau-bound cells were observed, but above 5 μM , more than 50% of cells were bound to Tau. Finally, we confirmed the effect of the aggregation inhibitor on membrane binding. Several compounds were identified that inhibited Tau aggregation. Among them, EGCG, a well-known aggregation inhibitor, was used to measure membrane binding changes in Tau aggregates⁵³⁻⁵⁵. EGCG efficiently inhibited Tau K18 aggregation (Figure 42) and reduced membrane binding of Tau K18 aggregates as the treatment dose increased^{35, 37, 54} (Figure 43A, B)

Membrane binding of Tau K18 in various cell lines

Membrane binding of Tau K18 aggregates appeared to occur throughout the cell and not at a specific location (Figure 44). We speculated that membrane binding of Tau K18 aggregates might occur in other cell lines. To confirm this hypothesis, hippocampal neuronal cell (HT22), glial cell (B103), bone marrow neuroblastoma (SH-SY5Y), and embryonic kidney cell (HEK293T) were treated with Tau K18 aggregates. Tau K18 aggregates bound to membranes in a dose-dependent manner in all cells regardless of the cell line (Figures 41 and 45). Binding affinity of Tau K18 aggregates to membranes was between 3 and 7 μ M and there was no significant difference between cell lines (Figure 46). Based on these results, it was expected that membrane binding of Tau K18 is a common phenomenon occurring in all cells rather than just binding to neuronal-specific cells.

Membrane binding of α -synuclein aggregates

α -synuclein is another well-known amyloid protein similar to Tau^{13, 56}
⁵⁷. α -synuclein aggregates can transmit into adjacent cells and induce misfolding and aggregation of α -synuclein similar to Tau propagation⁵⁸⁻⁶⁰. Owing to these similar features between α -synuclein and Tau, we suspected that α -synuclein would also bind to membranes based on aggregation. To verify this hypothesis, fluorescence labeled α -

synuclein aggregates were generated in the same manner as the Tau K18 mixture (Figure 47A, B). α -synuclein aggregates were treated with various concentrations (1, 5, and 10 μ M). α -synuclein bound to membranes as the amount of aggregates increased (Figure 48). Binding was observed in more than 40% of cells at 1 μ M and saturation of binding occurred at 5 μ M or more. These results showed that α -synuclein bound to membranes dependent on the amount of aggregates, which was similar to the Tau binding results.

Figure 33. Thioflavin T (ThT) fluorescence intensity of Tau K18 during aggregation

Tau K18 only and a mixture with labeled Tau K18 (100 μ M) were aggregated with 50 μ M ODS inducer. At each time point, samples were incubated with 50 μ M ThT and fluorescence measured.

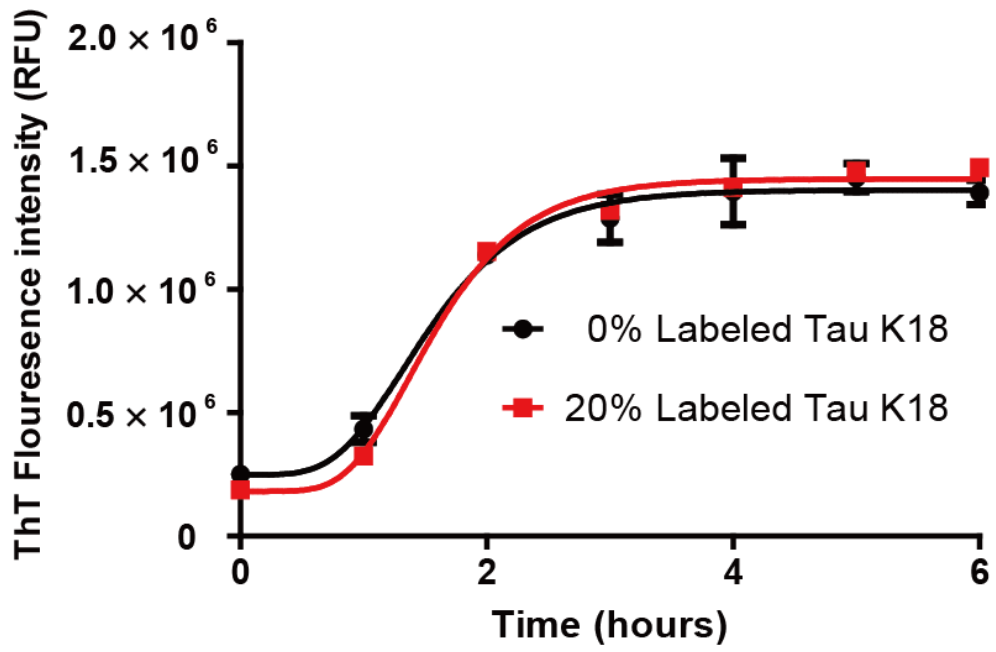
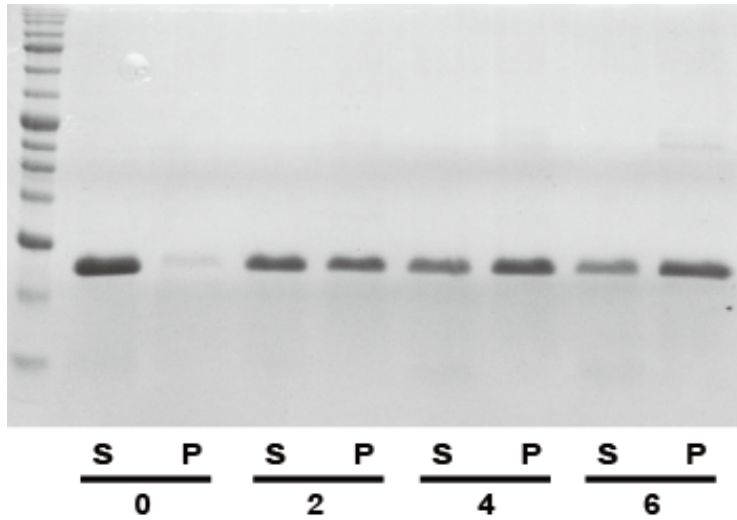


Figure 34. Sedimentation fraction of Tau K18 aggregates

(A) Aggregated mixtures with labeled Tau K18 (100 μ M) were centrifuged at $16,000 \times g$ for 15 min to generate a pellet fraction (P) and supernatants (S) every 2 hours. Separated samples were analyzed and visualized by 15% SDS-PAGE and Coomassie blue staining.

(B) Quantification of band intensities were measured with ImageJ software.

(A)



(B)

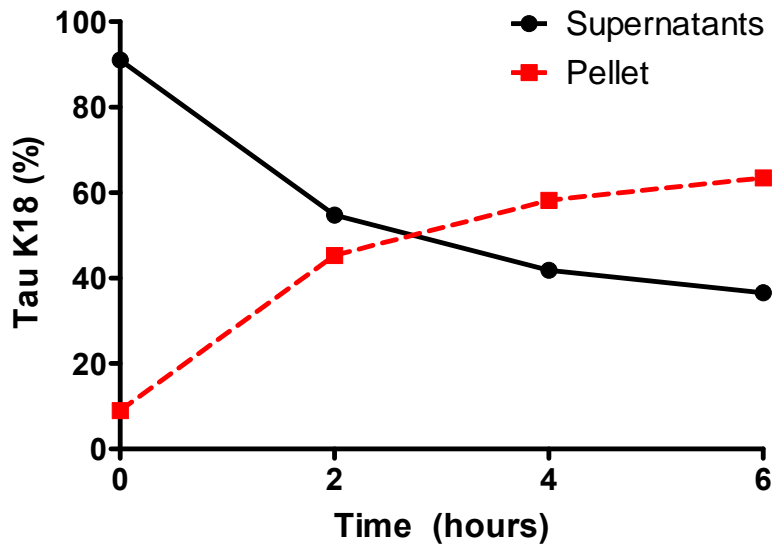
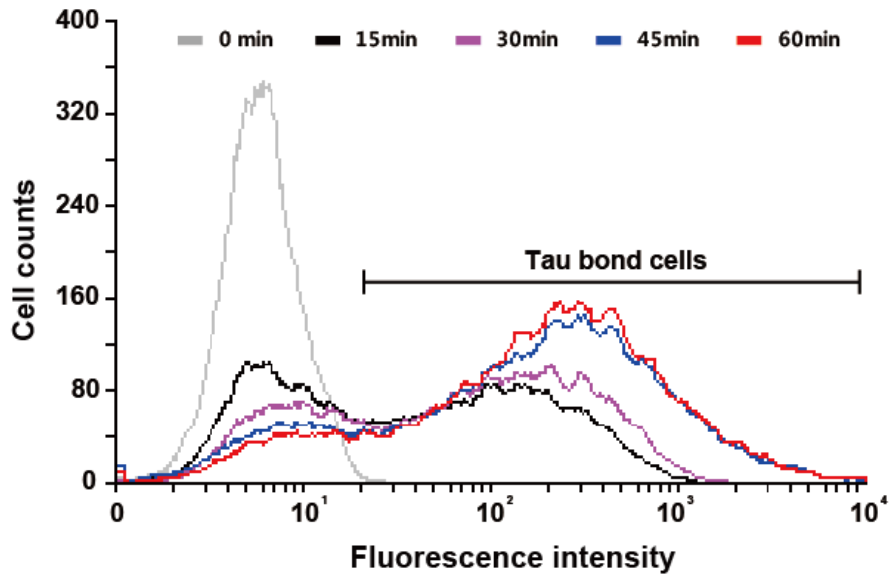


Figure 35. Flow cytometer histogram of the membrane bound Tau K18 by incubation time

(A) HT22 cells were treated at various times (15, 30, 45, and 60 min) with Tau K18 (10 μ M) aggregated for 6 hours. Each cell was washed with PBS buffer twice and membrane bound Tau K18 was detected by FACS analysis (approximately 20,000 cells per sample in three independent experiments).

(B) Percentage of Tau K18 bound cells in each population. The graph represents the cells bound with Tau K18 and untreated cells were used as a negative control. Data shown are the means \pm S.D. of three different experiments

(A)



(B)

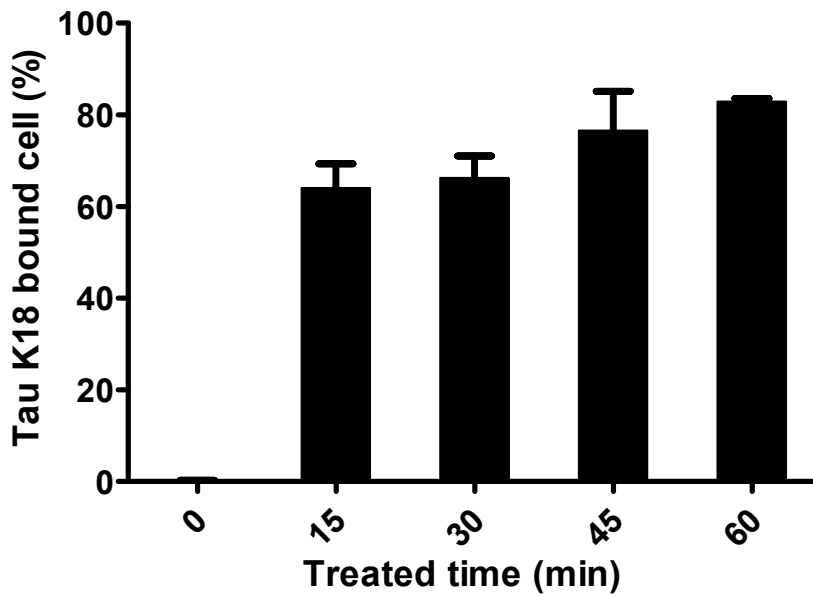
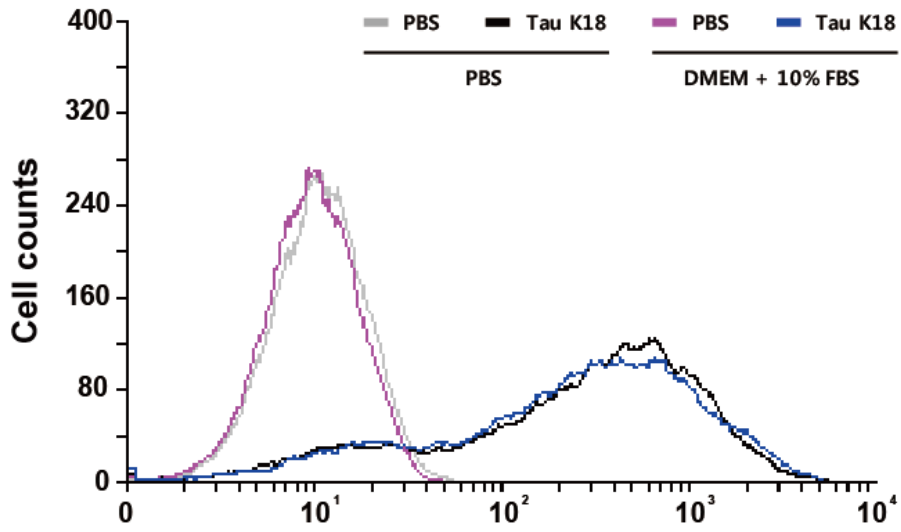


Figure 36. Membrane binding of Tau K18 in different buffer solutions

(A) Flow cytometer histogram of the membrane bound Tau K18 in different buffer solutions. Tau K18 aggregates (10 μ M) were incubated with HT22 cells for 1 hour in PBS or DMEM containing 10% FBS. Each cell was washed with PBS buffer twice and the Tau K18 remaining on membranes was detected by FACS analysis (approximately 20,000 cells per sample in three independent experiments).

(B) Percentage of Tau K18 bounded cells in each population. The graph represents cells bound with Tau K18 in different buffer solutions.

(A)



(B)

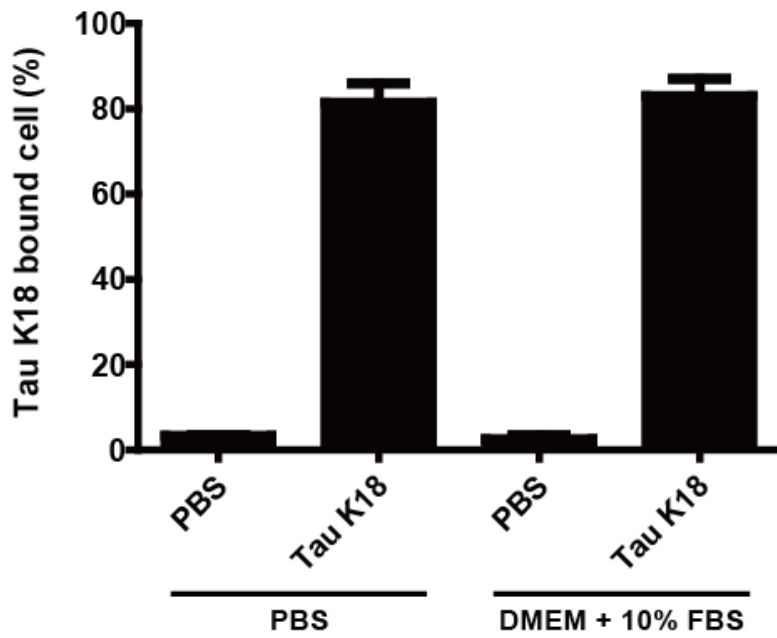
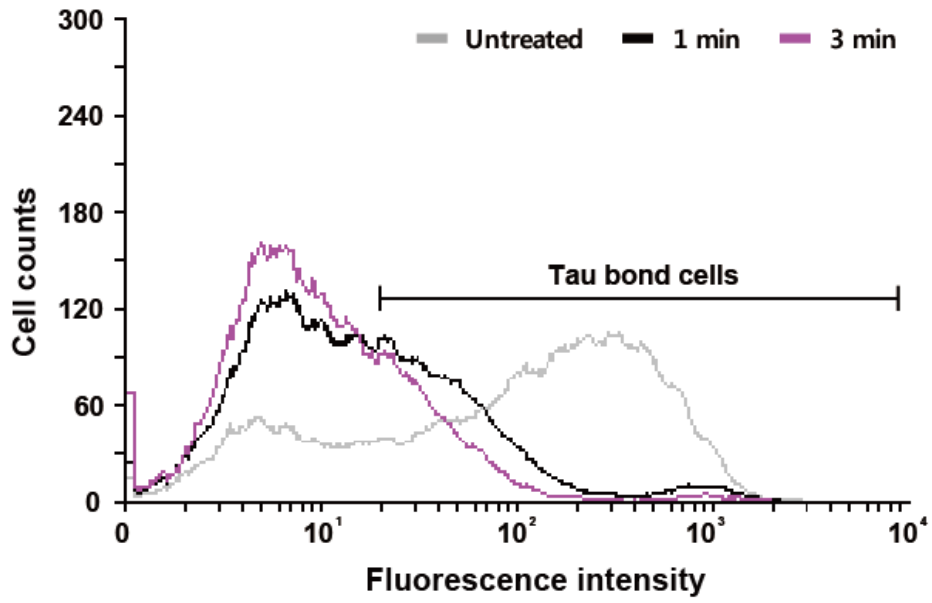


Figure 37. Flow cytometer histogram of membranes with remaining Tau K18 after trypsin treatment

(A) Tau K18 aggregates (10 μ M) were incubated with cells for 1 h and then 0.125% trypsin was added for 1 and 3 min at 37°C. Each cell was washed with PBS buffer twice and the remaining Tau K18 on the membranes was detected by FACS analysis (approximately 20,000 cells per sample in three independent experiments).

(B) Percentage of remaining Tau K18 on the cell membrane after the treatment time. The graph represents the remaining Tau K18 on the cell membrane.

(A)



(B)

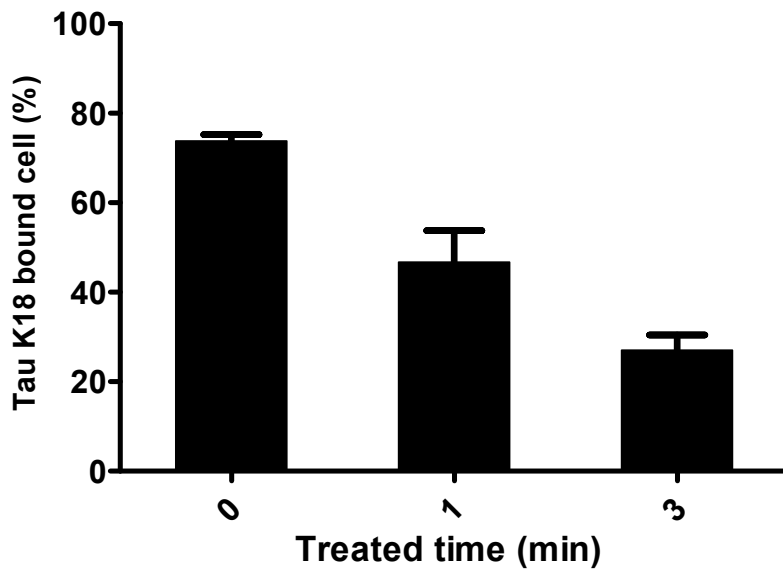


**Figure 38. Fluorescence microscopy images showing the remaining
Tau aggregates**

Cells were treated Tau K18 aggregates (10 μ M) for 1 hour, and then, 0.125% trypsin was added for 3 mins at 37 °C. Treated cells were washed with PBS buffer twice.

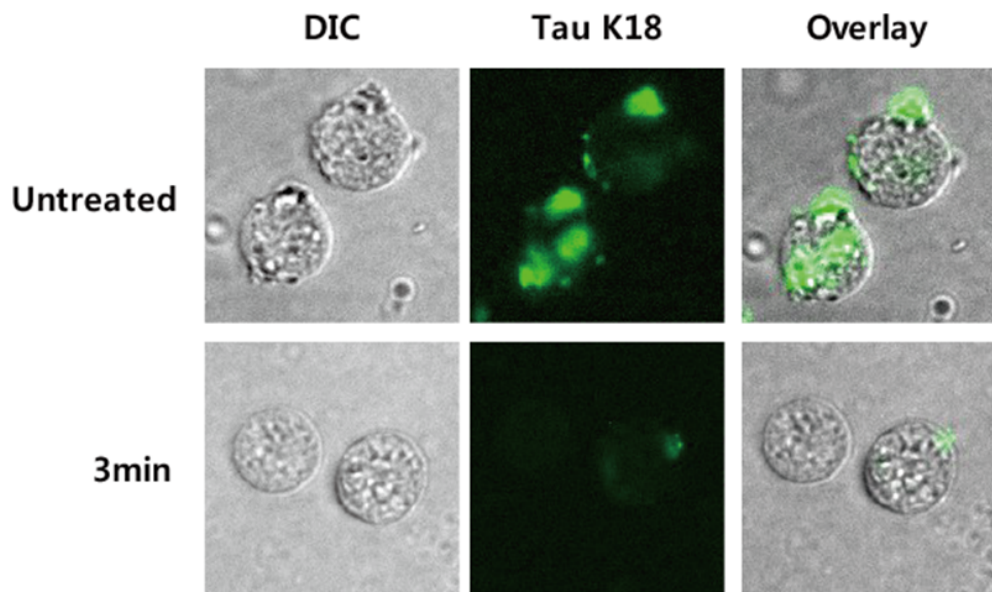


Figure 39. Degradation of Tau K18 aggregates with trypsin

An aggregated mixture with 20% labeled Tau K18 was treated with 0.125% trypsin for 1, 3, and 5 min and treated samples were visualized by 15% SDS-PAGE and Coomassie blue staining.

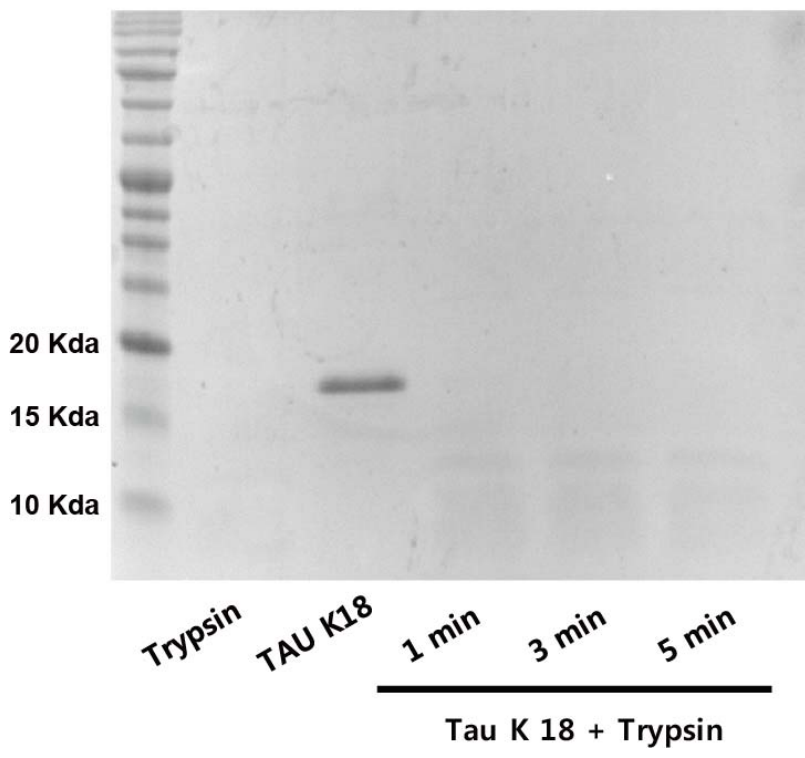
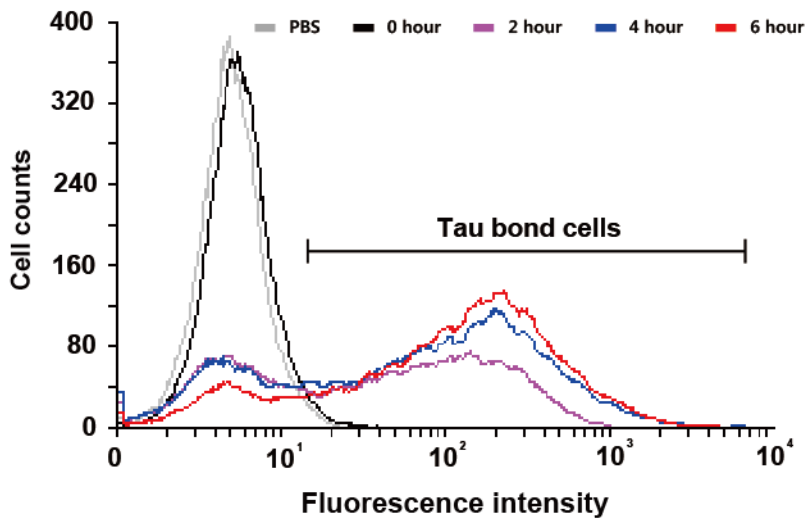


Figure 40. Flow cytometer histogram of membrane bound Tau K18 by aggregation time

(A) Tau K18 aggregates were collected every 2 hours and HT22 cells were treated with these aggregates (10 μ M) for 1 hour. Each cell was washed with PBS buffer twice and membrane bound Tau K18 was detected by FACS analysis (approximately 20,000 cells per sample in three independent experiments). (B) Percentage of Tau K18 bounded cells in each population. The graph represents cells bound with Tau K18 by aggregation time.

(A)



(B)

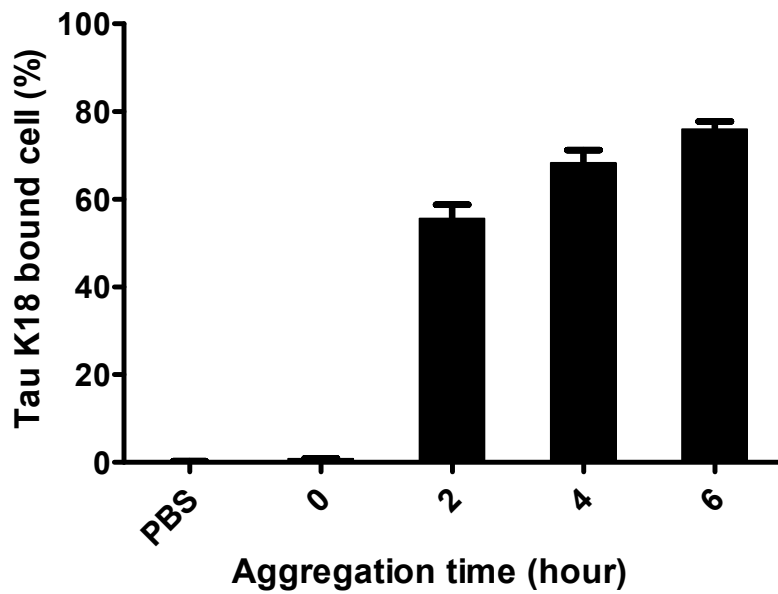
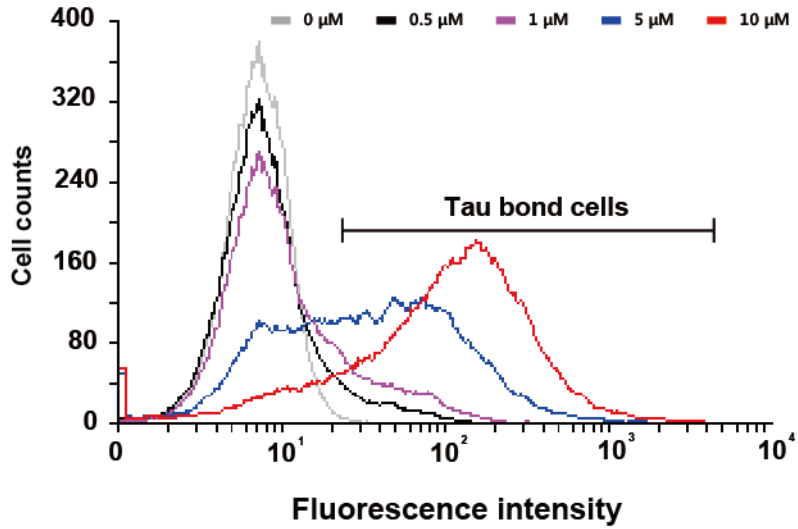


Figure 41. Flow cytometer histogram of membrane bound Tau K18 by treatment dose

(A) HT22 cells were treated with various concentrations (0, 0.5, 1, 5, and 10 μM) of Tau K18 aggregated for 6 hours. Each cell was washed with PBS buffer twice, and membrane bound Tau K18 was detected by FACS analysis (approximately 20,000 cells per sample in three independent experiments). (B) Percentage of Tau K18 bound cells in each population. The graph represents cells bound with Tau K18 according to the treatment dose.

(A)



(B)

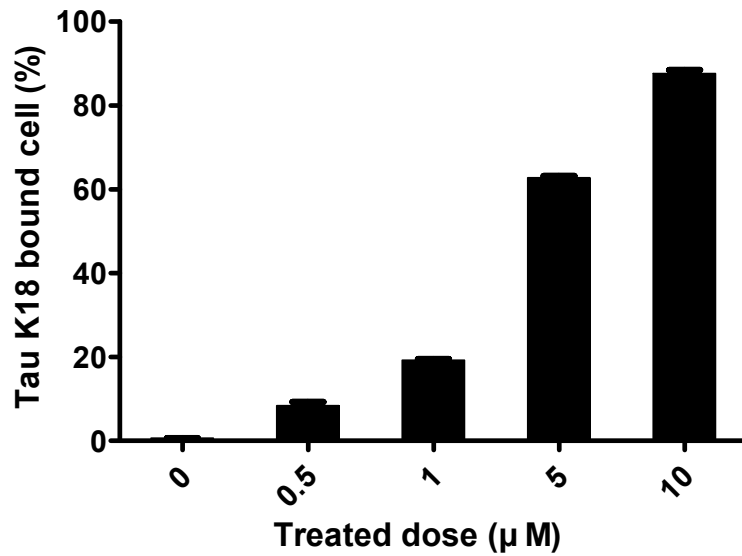
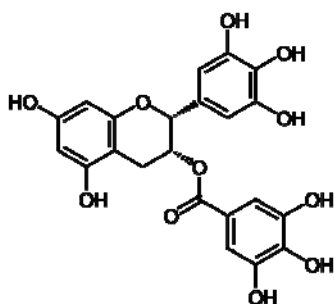


Figure 42. ThT fluorescence of the inhibitor treated Tau K18

(A) Structure of epigallocatechin gallate (EGCG)

(B) Tau K18 (100 μM) was aggregated with various concentrations of EGCG (10, 100, and 1000 μM) and immediately added to ThT to measure fluorescence.

(A)



(B)

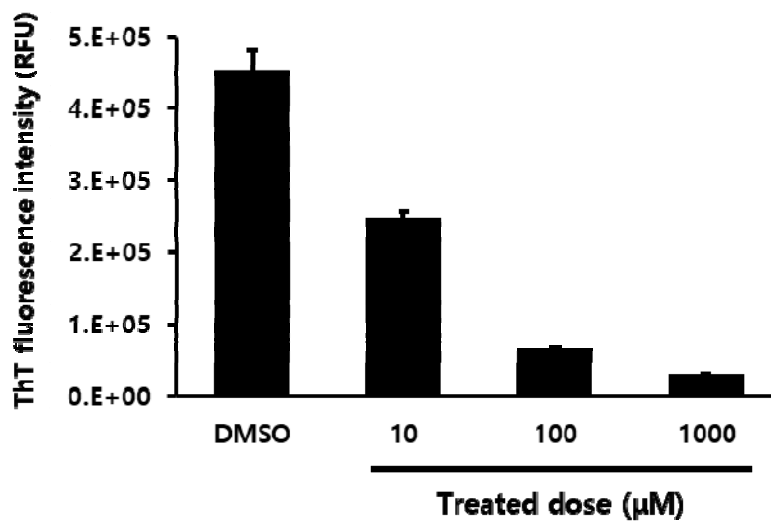
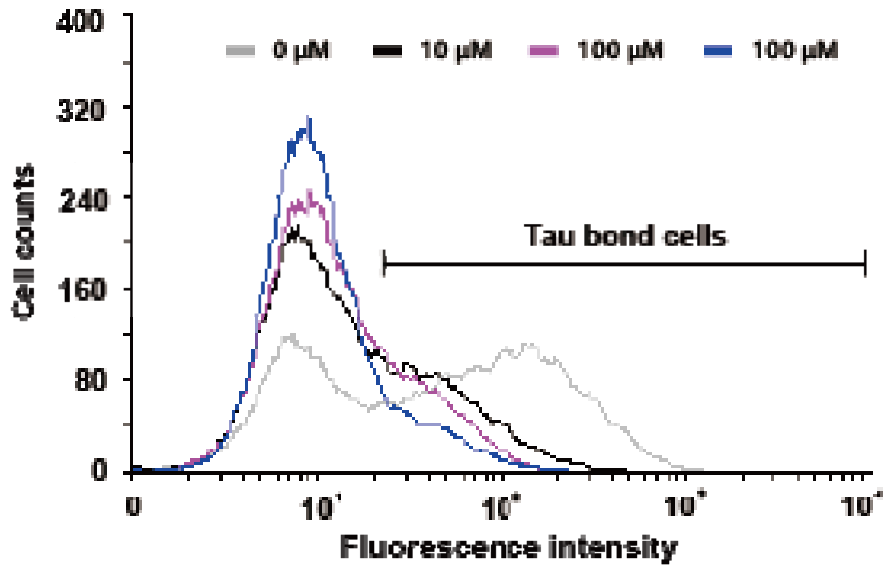


Figure 43. Reducing membrane binding by EGCG

(A) Flow cytometer histograms of the membrane bound Tau K18 treated with inhibitor. Tau K18 (100 μM) were aggregated with various concentrations of EGCG (10, 100, and 1000 μM) and these aggregates (5 μM) were mix with HT22 cells for 1 hour. The treated cells were washed with PBS twice and membrane bound Tau K18 was detected by FACS analysis (approximately 20,000 cells per sample in three independent experiments). (B) Percentage of Tau K18 bound cells in each population. The graph represents the degree of Tau K18 binding based on the concentration of inhibitor used.

(A)



(B)

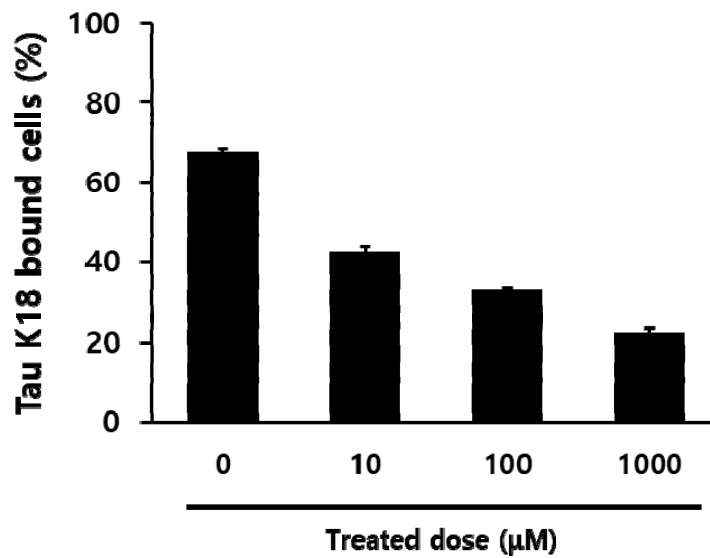


Figure 44. Fluorescence microscope images showing the membrane bound Tau K18

Cells were treated with various concentrations of Tau K18 aggregates (0, 0.5, 1, 5, and 10 μM). Treated cells were washed with PBS buffer twice.

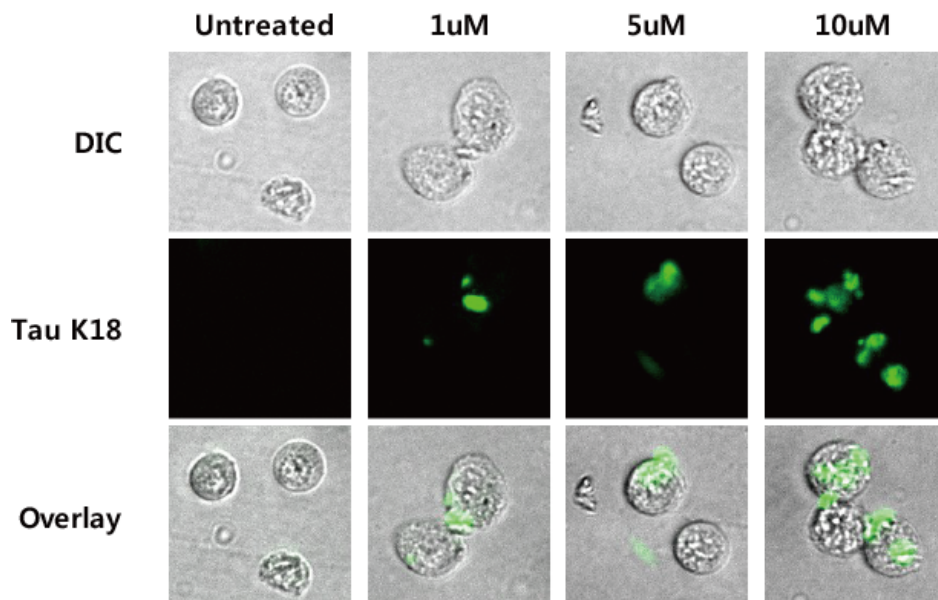


Figure 45. Cell line independent membrane binding of Tau K18

Flow cytometer histograms of membrane bound Tau K18 for SH-SY5Y, B103, and HEK293T. Each cell lines were was treated with Tau K18 aggregates for 1 hour. Each cell was washed with PBS buffer twice, and membrane bound Tau K18 was detected by FACS analysis (about approximately 20,000 cells per sample in three independent experiments).

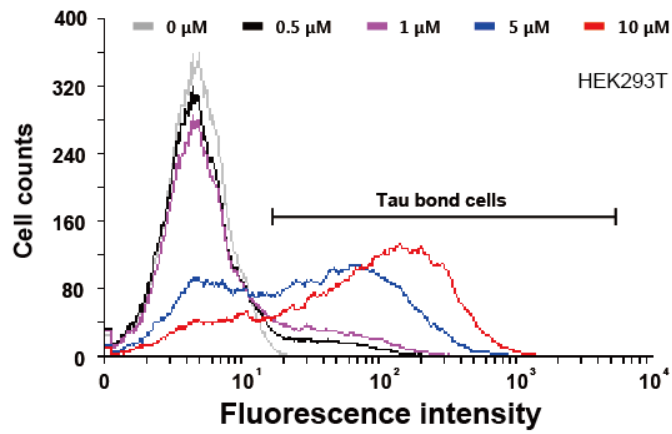
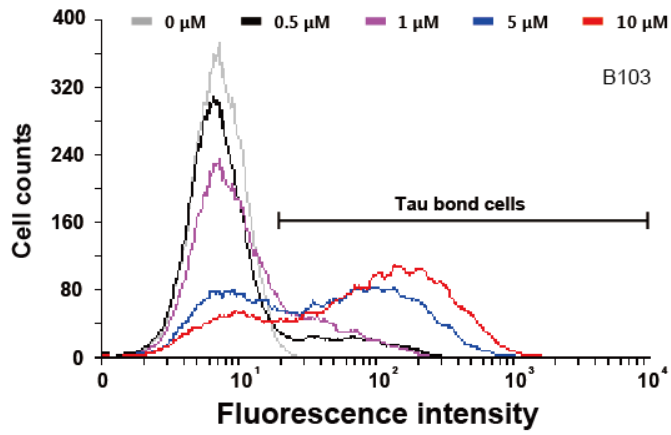
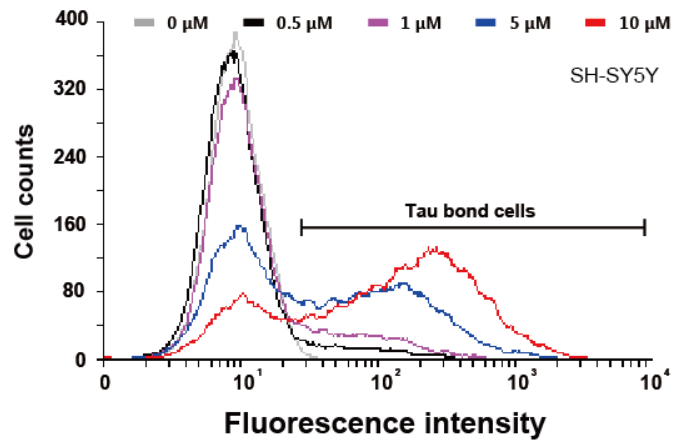


Figure 46. Comparing K_d values of Tau aggregates and cells

Change in ratio of Tau K18 aggregate -bound cells was plotted as a function of the ligand concentration to yield a comparable K_d value.

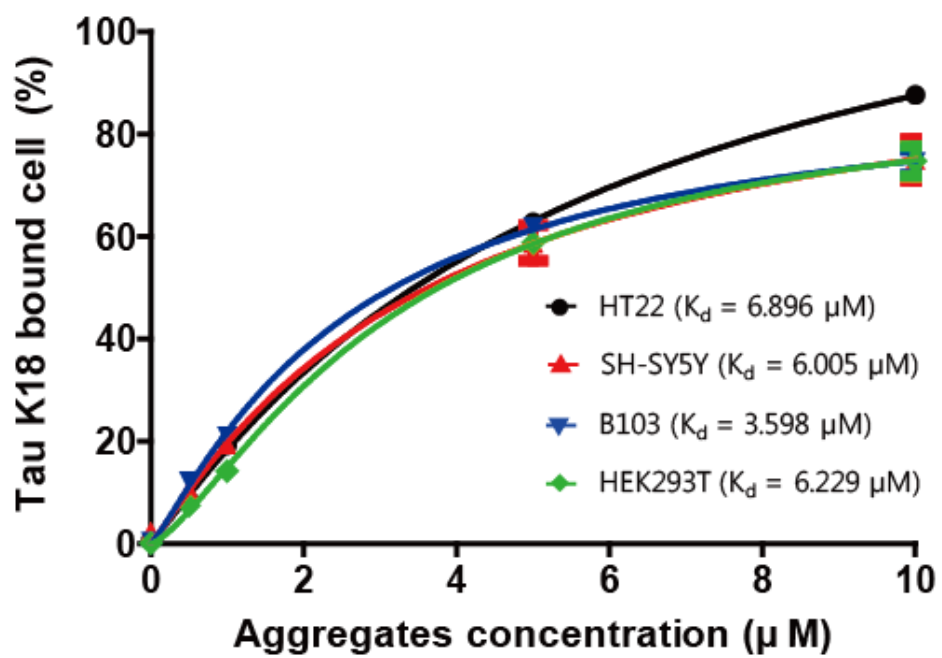


Figure 47. Aggregation kinetic α -synuclein in the presence of fluorescence labeled α -synuclein

ThT fluorescence intensity during aggregation. α -synuclein (80 μ M) was aggregated with 20 μ M labeled α -synuclein. At each time point, samples were incubated with 5 μ M ThT and fluorescence was measured.

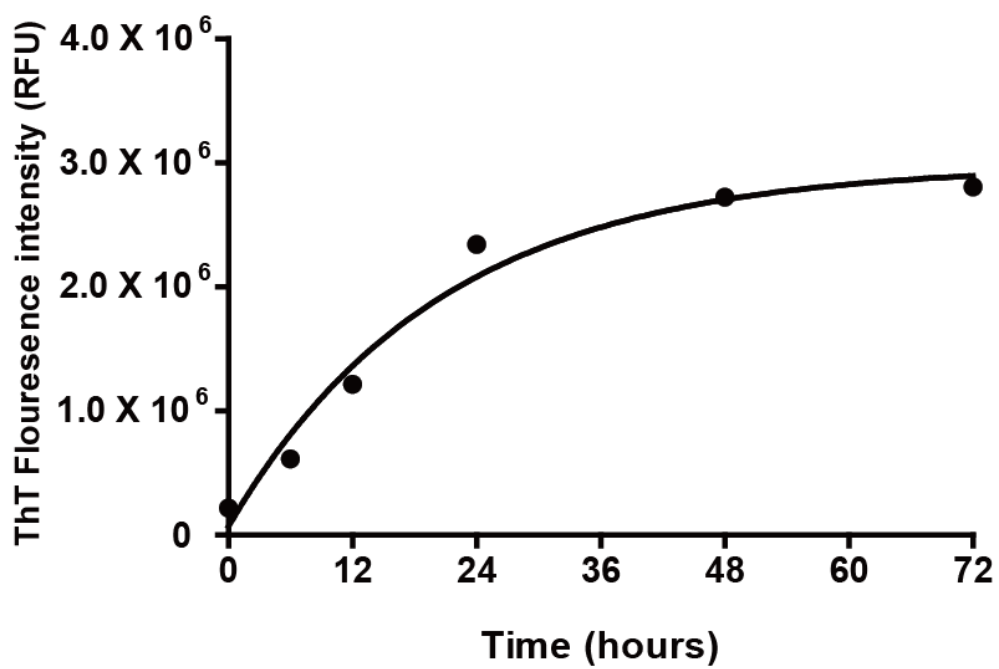
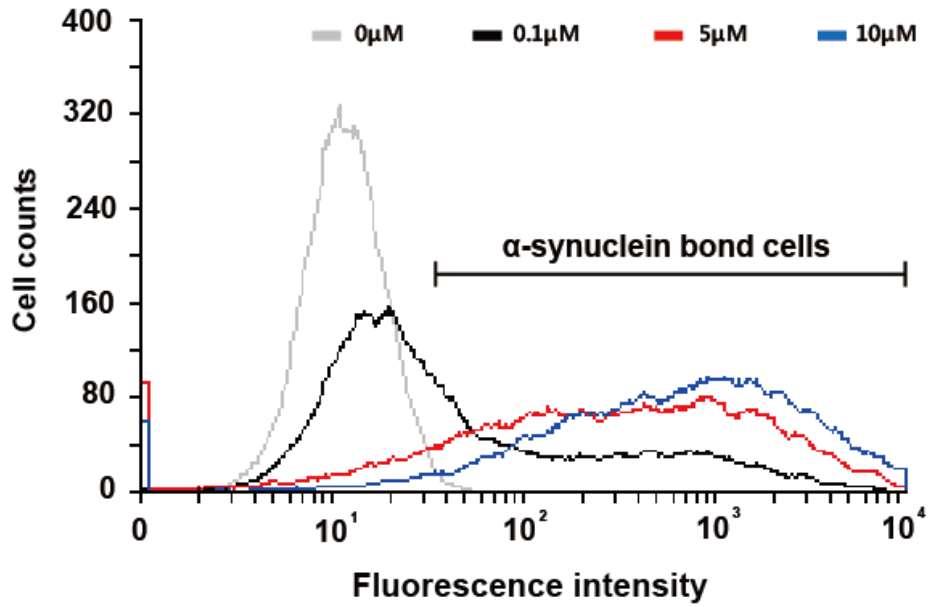


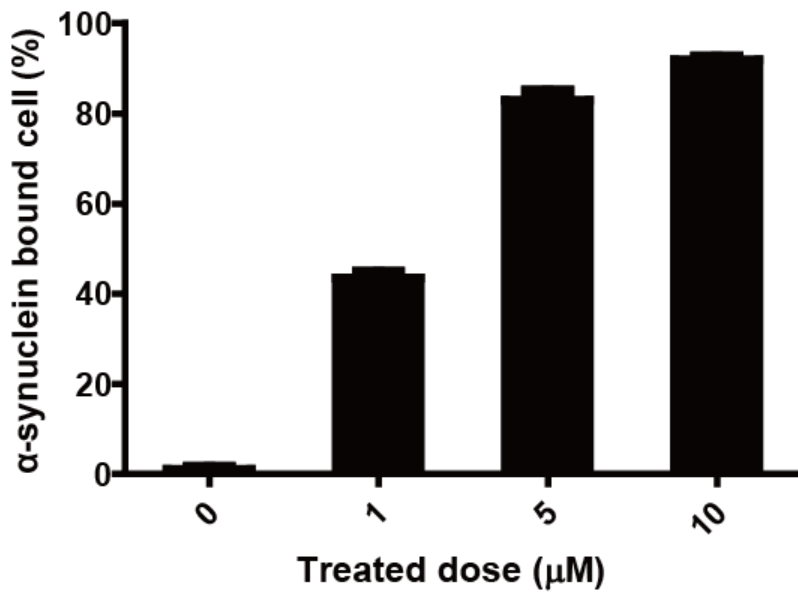
Figure 48. Membrane binding of aggregated α -synuclein by treated dose

(A) Flow cytometer histograms of membrane bound α -synuclein by treatment dose. HT22 cells were treated with various concentrations (0, 1, 5, and 10 μ M) of α -synuclein aggregated for 24 h. Each cell was washed with PBS buffer twice and membrane bound Tau K18 was detected by FACS analysis (approximately 20,000 cells per sample in three independent experiments). (B) Percentage of α -synuclein bound cells in each population. The graph represents the cells bound with α -synuclein based on the treatment dose.

(A)



(B)



DISCUSSION

Membrane mediated Tau transmission is an important factor in disease progression^{42, 61-62}. Measuring the membrane binding of Tau aggregates provides an important method for studying disease progression. We conventionally measured membrane binding under various conditions using fluorescence labeled Tau aggregates (Figures 33 and 34). As aggregation progressed, the amount of membrane bound Tau increased (Figure 35). This might be one factor that allowed cells to more easily uptake Tau^{43, 52 63}. In addition, Tau aggregates did not bind to cell membranes at specific locations and could bind to membranes in various neuronal cells (HT22, HEK293T, SH-SY5Y, and B103) (Figures 45 and 46). This non-specific binding suggests that the binding of Tau might not be cell or receptor specific. Recent studies have shown that heparan sulfate proteoglycans play an important role in the uptake of Tau aggregates^{43, 61}. Heparan sulfate proteoglycans are distributed in membranes of all cells, bind many ligands, regulate numerous cellular activities, and assist with tissue structure and physiology^{43, 64-65}. However, this non-specific binding still has important implications. Tau propagation was reduced when the uptake of Tau aggregates was inhibited via the use of antibodies^{42, 45, 66} and,

unlike other tissue cells, neuronal cells were more vulnerable to Tau aggregates because of higher levels of Tau expression than that in other cell lines ⁶⁷⁻⁶⁸. Finally, it was shown that measuring membrane binding could be extended not only to Tau but also to other amyloid proteins such as α -synuclein ⁶⁹⁻⁷¹. As the amount of α -synuclein aggregates increased, the proportion of membrane-bound cells increased.

In the present study, we were able to effectively measure membrane binding of Tau using fluorescently labeled Tau K18 as a probe. Binding of Tau was confirmed in several cells and this binding indicated that various cells could be platforms for measuring membrane binding. This method might be a good tool to screen or verify more efficient compounds or antibodies. It is also expected that this approach would be applicable to other amyloid proteins.

REFERENCES

1. Brettschneider, J.; Del Tredici, K.; Lee, V. M. Y.; Trojanowski, J. Q., Spreading of pathology in neurodegenerative diseases: a focus on human studies. *Nature reviews. Neuroscience* **2015**, *16* (2), 109–120.
2. de Calignon, A.; Polydoro, M.; Suárez-Calvet, M.; William, C.; Adamowicz, David H.; Kopeikina, Kathy J.; Pitstick, R.; Sahara, N.; Ashe, Karen H.; Carlson, George A.; Spires-Jones, Tara L.; Hyman, Bradley T., Propagation of Tau Pathology in a Model of Early Alzheimer's Disease. *Neuron* **2012**, *73* (4), 685–697.
3. Mietelska-Porowska, A.; Wasik, U.; Goras, M.; Filipek, A.; Niewiadomska, G., Tau Protein Modifications and Interactions: Their Role in Function and Dysfunction. *International Journal of Molecular Sciences* **2014**, *15* (3), 4671–4713.
4. Iqbal, K.; Liu, F.; Gong, C. X., Tau and neurodegenerative disease: the story so far. *Nature reviews. Neurology* **2016**, *12* (1), 15–27.
5. Wang, Y.; Mandelkow, E., Tau in physiology and pathology. *Nat Rev Neurosci* **2016**, *17* (1), 5–21.
6. Drubin, D. G.; Kirschner, M. W., Tau protein function in

living cells. *The Journal of cell biology* **1986**, *103* (6 Pt 2), 2739-46.

7. Feinstein, S. C.; Wilson, L., Inability of tau to properly regulate neuronal microtubule dynamics: a loss-of-function mechanism by which tau might mediate neuronal cell death. *Biochim Biophys Acta* **2005**, *1739* (2-3), 268-79.

8. Alonso, A. C.; Zaidi, T.; Grundke-Iqbal, I.; Iqbal, K., Role of abnormally phosphorylated tau in the breakdown of microtubules in Alzheimer disease. *Proceedings of the National Academy of Sciences of the United States of America* **1994**, *91* (12), 5562-5566.

9. Flach, K.; Hilbrich, I.; Schiffmann, A.; Gartner, U.; Kruger, M.; Leonhardt, M.; Waschipky, H.; Wick, L.; Arendt, T.; Holzer, M., Tau oligomers impair artificial membrane integrity and cellular viability. *J Biol Chem* **2012**, *287* (52), 43223-33.

10. Li, X.-C.; Hu, Y.; Wang, Z.-h.; Luo, Y.; Zhang, Y.; Liu, X.-P.; Feng, Q.; Wang, Q.; Ye, K.; Liu, G.-P.; Wang, J.-Z., Human wild-type full-length tau accumulation disrupts mitochondrial dynamics and the functions via increasing mitofusins. *Scientific Reports* **2016**, *6*, 24756.

11. Guo, J. L.; Lee, V. M., Cell-to-cell transmission of

pathogenic proteins in neurodegenerative diseases. *Nature medicine* **2014**, *20* (2), 130-8.

12. Iba, M.; Guo, J. L.; McBride, J. D.; Zhang, B.; Trojanowski, J. Q.; Lee, V. M., Synthetic tau fibrils mediate transmission of neurofibrillary tangles in a transgenic mouse model of Alzheimer's-like tauopathy. *The Journal of neuroscience : the official journal of the Society for Neuroscience* **2013**, *33* (3), 1024-37.

13. Jucker, M.; Walker, L. C., Self-propagation of pathogenic protein aggregates in neurodegenerative diseases. *Nature* **2013**, *501* (7465), 45-51.

14. Lovestone, S.; Boada, M.; Dubois, B.; Hull, M.; Rinne, J. O.; Huppertz, H. J.; Calero, M.; Andres, M. V.; Gomez-Carrillo, B.; Leon, T.; del Ser, T., A phase II trial of tideglusib in Alzheimer's disease. *Journal of Alzheimer's disease : JAD* **2015**, *45* (1), 75-88.

15. Medina, M.; Avila, J., New perspectives on the role of tau in Alzheimer's disease. Implications for therapy. *Biochemical Pharmacology* **2014**, *88* (4), 540-547.

16. Taniguchi, S.; Suzuki, N.; Masuda, M.; Hisanaga, S.; Iwatsubo, T.; Goedert, M.; Hasegawa, M., Inhibition of heparin-induced tau filament formation by phenothiazines, polyphenols,

- and porphyrins. *J Biol Chem* **2005**, *280* (9), 7614–23.
17. Taghavi, A.; Nasir, S.; Pickhardt, M.; Heyny-von Haussen, R.; Mall, G.; Mandelkow, E.; Mandelkow, E. M.; Schmidt, B., N'-benzylidene-benzohydrazides as novel and selective tau-PHF ligands. *Journal of Alzheimer's disease : JAD* **2011**, *27* (4), 835–43.
18. Wang, C. K.; Northfield, S. E.; Huang, Y. H.; Ramos, M. C.; Craik, D. J., Inhibition of tau aggregation using a naturally-occurring cyclic peptide scaffold. *European journal of medicinal chemistry* **2016**, *109*, 342–9.
19. Nadimidla, K.; Ismail, T.; Kanapathipillai, M., Tau peptides and tau mutant protein aggregation inhibition by cationic polyethyleneimine and polyarginine. *Biopolymers* **2017**, *107* (9).
20. Kim, Y.; Park, J. H.; Lee, H.; Nam, J. M., How Do the Size, Charge and Shape of Nanoparticles Affect Amyloid beta Aggregation on Brain Lipid Bilayer? *Sci Rep* **2016**, *6*, 19548.
21. Liu, H.; Xie, B.; Dong, X.; Zhang, L.; Wang, Y.; Liu, F.; Sun, Y., Negatively charged hydrophobic nanoparticles inhibit amyloid β -protein fibrillation: The presence of an optimal charge density. *Reactive and Functional Polymers* **2016**, *103*, 108–116.
22. Hawe, A.; Sutter, M.; Jiskoot, W., Extrinsic Fluorescent Dyes as Tools for Protein Characterization. *Pharmaceutical*

Research **2008**, *25* (7), 1487-1499.

23. Younan, N. D.; Viles, J. H., A Comparison of Three Fluorophores for the Detection of Amyloid Fibers and Prefibrillar Oligomeric Assemblies. ThT (Thioflavin T); ANS (1-Anilinonaphthalene-8-sulfonic Acid); and bisANS (4,4'-Dianilino-1,1'-binaphthyl-5,5'-disulfonic Acid). *Biochemistry* **2015**, *54* (28), 4297-306.

24. Bulic, B.; Pickhardt, M.; Mandelkow, E., Progress and developments in tau aggregation inhibitors for Alzheimer disease. *Journal of medicinal chemistry* **2013**, *56* (11), 4135-55.

25. Kokkoni, N.; Stott, K.; Amijee, H.; Mason, J. M.; Doig, A. J., N-Methylated Peptide Inhibitors of β -Amyloid Aggregation and Toxicity. Optimization of the Inhibitor Structure. *Biochemistry* **2006**, *45* (32), 9906-9918.

26. Ladiwala, A. R.; Lin, J. C.; Bale, S. S.; Marcelino-Cruz, A. M.; Bhattacharya, M.; Dordick, J. S.; Tessier, P. M., Resveratrol selectively remodels soluble oligomers and fibrils of amyloid Abeta into off-pathway conformers. *J Biol Chem* **2010**, *285* (31), 24228-37.

27. Chen, J. X.; Yan, S. D., Amyloid-beta-induced mitochondrial dysfunction. *Journal of Alzheimer's disease : JAD*

2007, *12* (2), 177–84.

28. Kamp, F.; Exner, N.; Lutz, A. K.; Wender, N.; Hegermann, J.; Brunner, B.; Nuscher, B.; Bartels, T.; Giese, A.; Beyer, K.; Eimer, S.; Winklhofer, K. F.; Haass, C., Inhibition of mitochondrial fusion by alpha-synuclein is rescued by PINK1, Parkin and DJ-1. *The EMBO journal* **2010**, *29* (20), 3571–89.

29. Watanabe, H.; Ono, M.; Ariyoshi, T.; Katayanagi, R.; Saji, H., Novel Benzothiazole Derivatives as Fluorescent Probes for Detection of β -Amyloid and α -Synuclein Aggregates. *ACS chemical neuroscience* **2017**, *8* (8), 1656–1662.

30. Gillam, J. E.; MacPhee, C. E., Modelling amyloid fibril formation kinetics: mechanisms of nucleation and growth. *Journal of physics. Condensed matter : an Institute of Physics journal* **2013**, *25* (37), 373101.

31. Arosio, P.; Knowles, T. P.; Linse, S., On the lag phase in amyloid fibril formation. *Physical chemistry chemical physics : PCCP* **2015**, *17* (12), 7606–18.

32. Clavaguera, F.; Bolmont, T.; Crowther, R. A.; Abramowski, D.; Frank, S.; Probst, A.; Fraser, G.; Stalder, A. K.; Beibel, M.; Staufenbiel, M.; Jucker, M.; Goedert, M.; Tolnay, M., Transmission and spreading of tauopathy in transgenic mouse

brain. *Nature cell biology* **2009**, *11* (7), 909–913.

33. Holmes, B. B.; Furman, J. L.; Mahan, T. E.; Yamasaki, T. R.; Mirbaha, H.; Eades, W. C.; Belaygorod, L.; Cairns, N. J.; Holtzman, D. M.; Diamond, M. I., Proteopathic tau seeding predicts tauopathy in vivo. *Proceedings of the National Academy of Sciences of the United States of America* **2014**, *111* (41), E4376–E4385.

34. Shammas, S. L.; Garcia, G. A.; Kumar, S.; Kjaergaard, M.; Horrocks, M. H.; Shivji, N.; Mandelkow, E.; Knowles, T. P.; Mandelkow, E.; Klenerman, D., A mechanistic model of tau amyloid aggregation based on direct observation of oligomers. *Nature communications* **2015**, *6*, 7025.

35. Du, W. J.; Guo, J. J.; Gao, M. T.; Hu, S. Q.; Dong, X. Y.; Han, Y. F.; Liu, F. F.; Jiang, S.; Sun, Y., Brazilin inhibits amyloid beta-protein fibrillogenesis, remodels amyloid fibrils and reduces amyloid cytotoxicity. *Sci Rep* **2015**, *5*, 7992.

36. Palhano, F. L.; Lee, J.; Grimster, N. P.; Kelly, J. W., Toward the molecular mechanism(s) by which EGCG treatment remodels mature amyloid fibrils. *Journal of the American Chemical Society* **2013**, *135* (20), 7503–10.

37. Wobst, H. J.; Sharma, A.; Diamond, M. I.; Wanker, E. E.;

Bieschke, J., The green tea polyphenol (-)-epigallocatechin gallate prevents the aggregation of tau protein into toxic oligomers at substoichiometric ratios. *FEBS letters* **2015**, *589* (1), 77-83.

38. Roostae, A.; Beaudoin, S.; Staskevicius, A.; Roucou, X., Aggregation and neurotoxicity of recombinant α -synuclein aggregates initiated by dimerization. *Molecular Neurodegeneration* **2013**, *8* (1), 5.

39. Chaturvedi, S. K.; Siddiqi, M. K.; Alam, P.; Khan, R. H., Protein misfolding and aggregation: Mechanism, factors and detection. *Process Biochemistry* **2016**, *51* (9), 1183-1192.

40. Ross, C. A.; Poirier, M. A., Protein aggregation and neurodegenerative disease. *Nature medicine* **2004**, *10 Suppl*, S10-7.

41. Bandyopadhyay, B.; Li, G.; Yin, H.; Kuret, J., Tau aggregation and toxicity in a cell culture model of tauopathy. *J Biol Chem* **2007**, *282* (22), 16454-64.

42. Kfoury, N.; Holmes, B. B.; Jiang, H.; Holtzman, D. M.; Diamond, M. I., Trans-cellular propagation of Tau aggregation by fibrillar species. *J Biol Chem* **2012**, *287* (23), 19440-51.

43. Holmes, B. B.; DeVos, S. L.; Kfoury, N.; Li, M.; Jacks, R.;

Yanamandra, K.; Ouidja, M. O.; Brodsky, F. M.; Marasa, J.; Bagchi, D. P.; Kotzbauer, P. T.; Miller, T. M.; Papy-Garcia, D.; Diamond, M. I., Heparan sulfate proteoglycans mediate internalization and propagation of specific proteopathic seeds. *Proceedings of the National Academy of Sciences of the United States of America* **2013**, *110* (33), E3138-47.

44. Wesen, E.; Jeffries, G. D. M.; Matson Dzebo, M.; Esbjorner, E. K., Endocytic uptake of monomeric amyloid-beta peptides is clathrin- and dynamin-independent and results in selective accumulation of Abeta(1-42) compared to Abeta(1-40). *Sci Rep* **2017**, *7* (1), 2021.

45. Agadjanyan, M. G.; Zagorski, K.; Petrushina, I.; Davtyan, H.; Kazarian, K.; Antonenko, M.; Davis, J.; Bon, C.; Blurton-Jones, M.; Cribbs, D. H.; Ghochikyan, A., Humanized monoclonal antibody armanezumab specific to N-terminus of pathological tau: characterization and therapeutic potency. *Molecular Neurodegeneration* **2017**, *12* (1), 33.

46. Yanamandra, K.; Jiang, H.; Mahan, T. E.; Maloney, S. E.; Wozniak, D. F.; Diamond, M. I.; Holtzman, D. M., Anti-tau antibody reduces insoluble tau and decreases brain atrophy. *Annals of Clinical and Translational Neurology* **2015**, *2* (3), 278-288.

47. Honson, N. S.; Jensen, J. R.; Darby, M. V.; Kuret, J., Potent inhibition of tau fibrillization with a multivalent ligand. *Biochemical and biophysical research communications* **2007**, *363* (1), 229-234.
48. Schafer, K. N.; Cisek, K.; Huseby, C. J.; Chang, E.; Kuret, J., Structural determinants of Tau aggregation inhibitor potency. *J Biol Chem* **2013**, *288* (45), 32599-611.
49. Biancalana, M.; Koide, S., Molecular Mechanism of Thioflavin-T Binding to Amyloid Fibrils. *Biochimica et biophysica acta* **2010**, *1804* (7), 1405-1412.
50. Khurana, R.; Coleman, C.; Ionescu-Zanetti, C.; Carter, S. A.; Krishna, V.; Grover, R. K.; Roy, R.; Singh, S., Mechanism of thioflavin T binding to amyloid fibrils. *Journal of Structural Biology* **2005**, *151* (3), 229-238.
51. Wolkers, W. F.; Looper, S. A.; Fontanilla, R. A.; Tsvetkova, N. M.; Tablin, F.; Crowe, J. H., Temperature dependence of fluid phase endocytosis coincides with membrane properties of pig platelets. *Biochimica et Biophysica Acta (BBA) - Biomembranes* **2003**, *1612* (2), 154-163.
52. Frost, B.; Jacks, R. L.; Diamond, M. I., Propagation of tau misfolding from the outside to the inside of a cell. *J Biol Chem*

2009, *284* (19), 12845–52.

53. Bieschke, J., Natural Compounds May Open New Routes to Treatment of Amyloid Diseases. *Neurotherapeutics* **2013**, *10* (3), 429–439.

54. Bieschke, J.; Russ, J.; Friedrich, R. P.; Ehrnhoefer, D. E.; Wobst, H.; Neugebauer, K.; Wanker, E. E., EGCG remodels mature alpha-synuclein and amyloid-beta fibrils and reduces cellular toxicity. *Proceedings of the National Academy of Sciences of the United States of America* **2010**, *107* (17), 7710–5.

55. Wang, Y.; Latshaw, D. C.; Hall, C. K., Aggregation of A β (17–36) in the Presence of Naturally Occurring Phenolic Inhibitors Using Coarse-Grained Simulations. *Journal of Molecular Biology* **2017**, *429* (24), 3893–3908.

56. Goedert, M.; Spillantini, M. G.; Del Tredici, K.; Braak, H., 100 years of Lewy pathology. *Nature reviews. Neurology* **2013**, *9* (1), 13–24.

57. Iljina, M.; Garcia, G. A.; Horrocks, M. H.; Tosatto, L.; Choi, M. L.; Ganzinger, K. A.; Abramov, A. Y.; Gandhi, S.; Wood, N. W.; Cremades, N.; Dobson, C. M.; Knowles, T. P.; Klenerman, D., Kinetic model of the aggregation of alpha-synuclein provides insights into prion-like spreading. *Proceedings of the National*

Academy of Sciences of the United States of America **2016**, *113* (9), E1206-15.

58. Luk, K. C.; Kehm, V.; Carroll, J.; Zhang, B.; O'Brien, P.; Trojanowski, J. Q.; Lee, V. M.-Y., Pathological α -Synuclein Transmission Initiates Parkinson-like Neurodegeneration in Nontransgenic Mice. *Science (New York, N.Y.)* **2012**, *338* (6109), 949-953.

59. Luk, K. C.; Song, C.; O'Brien, P.; Stieber, A.; Branch, J. R.; Brunden, K. R.; Trojanowski, J. Q.; Lee, V. M.-Y., Exogenous α -synuclein fibrils seed the formation of Lewy body-like intracellular inclusions in cultured cells. *Proceedings of the National Academy of Sciences* **2009**, *106* (47), 20051-20056.

60. Tran, H. T.; Chung, C. H.-Y.; Iba, M.; Zhang, B.; Trojanowski, J. Q.; Luk, K. C.; Lee, V. M. Y., α -Synuclein Immunotherapy Blocks Uptake and Templated Propagation of Misfolded α -Synuclein and Neurodegeneration. *Cell reports* **2014**, *7* (6), 2054-2065.

61. Mirbaha, H.; Holmes, B. B.; Sanders, D. W.; Bieschke, J.; Diamond, M. I., Tau Trimers Are the Minimal Propagation Unit Spontaneously Internalized to Seed Intracellular Aggregation. *The Journal of Biological Chemistry* **2015**, *290* (24), 14893-14903.

62. Wu, J. W.; Herman, M.; Liu, L.; Simoes, S.; Acker, C. M.; Figueroa, H.; Steinberg, J. I.; Margittai, M.; Kaye, R.; Zurzolo, C.; Di Paolo, G.; Duff, K. E., Small misfolded Tau species are internalized via bulk endocytosis and anterogradely and retrogradely transported in neurons. *J Biol Chem* **2013**, *288* (3), 1856-70.
63. Takeda, S.; Wegmann, S.; Cho, H.; DeVos, S. L.; Commins, C.; Roe, A. D.; Nicholls, S. B.; Carlson, G. A.; Pitstick, R.; Nobuhara, C. K.; Costantino, I.; Frosch, M. P.; Muller, D. J.; Irimia, D.; Hyman, B. T., Neuronal uptake and propagation of a rare phosphorylated high-molecular-weight tau derived from Alzheimer's disease brain. *Nature communications* **2015**, *6*, 8490.
64. Lin, X., Functions of heparan sulfate proteoglycans in cell signaling during development. *Development (Cambridge, England)* **2004**, *131* (24), 6009-21.
65. Sarrazin, S.; Lamanna, W. C.; Esko, J. D., Heparan Sulfate Proteoglycans. *Cold Spring Harbor Perspectives in Biology* **2011**, *3* (7), a004952.
66. Funk, K. E.; Mirbaha, H.; Jiang, H.; Holtzman, D. M.; Diamond, M. I., Distinct Therapeutic Mechanisms of Tau Antibodies: PROMOTING MICROGLIAL CLEARANCE VERSUS

BLOCKING NEURONAL UPTAKE. *The Journal of Biological Chemistry* **2015**, *290* (35), 21652–21662.

67. Freer, R.; Sormanni, P.; Vecchi, G.; Ciryam, P.; Dobson, C. M.; Vendruscolo, M., A protein homeostasis signature in healthy brains recapitulates tissue vulnerability to Alzheimer's disease. *Science Advances* **2016**, *2* (8).

68. Scholz, T.; Mandelkow, E., Transport and diffusion of Tau protein in neurons. *Cellular and molecular life sciences : CMLS* **2014**, *71* (16), 3139–50.

69. Aguzzi, A.; Lakkaraju, A. K., Cell Biology of Prions and Prionoids: A Status Report. *Trends in cell biology* **2016**, *26* (1), 40–51.

70. Goedert, M., Alzheimer's and Parkinson's diseases: The prion concept in relation to assembled A β , tau, and α -synuclein. *Science (New York, N.Y.)* **2015**, *349* (6248).

71. Lv, Z. Y.; Tan, C. C.; Yu, J. T.; Tan, L., Spreading of Pathology in Alzheimer's Disease. *Neurotoxicity research* **2017**.

국 문 초 록

Tau 응집체의 새로운 억제제와 막 결합에 관한 연구

Tau는 미세 소관을 안정화시키는 세포 내 미세 소관 관련 단백질입니다. 생리 조건에서, Tau는 본래 펼쳐진 단백질 및 높은 수용성 단백질입니다. 그러나 알츠하이머 병에서 Tau는 과인산화되어 NFT로 응집됩니다. 이 응집된 Tau는 인접한 세포로 전달되어 응집을 유도할 수 있습니다. 이 프리온과 같은 타우 증식은 질병 진행의 중요한 메커니즘으로 간주됩니다. 따라서, Tau의 응집 및 전달의 저해는 AD에 대한 치료제의 중요한 전략을 제공할 수 있다. 여기, 우리는 타우 (Tau) 응집을 위한 6 가지의 새로운 억제제를 선별하였고 선별된 화합물 구조에 기초한 1 개의 새로운 억제제를 디자인하였다. 이를 기반으로 62 개의 화합물이 합성되었고 32 개의 화합물이 타우 응집을 효과적으로 억제하였다. 또한, 우리는 응집된 Tau의 막 결합을 위한 새로운 측정 방법을 개발했습니다. 응집 의존적인 세포막 결합을 측정하기 위해, 형광 표지 된 타우가 사용되었다. Tau는 응집과 용량 의존적으로 살아있는 세포막에 결합합니다. 또한, EGCG 같은 응집 억제제를 사용함으로써, 본 방법은 막 결합 억제제의 확인 또는 스크리닝을 위한 편리한 세포 기반 접근법 일 수 있다는 것을 확인했다.

Keywords : 타우, 응집, 알츠하이머 질환, 저해제, 세포막 결합, FACS, 측정

Student number : 2009-30089